Universidade de Aveiro
2019

Departamento de Ciências Médicas

ANA ISABEL BAIÃO VIEIRA

Nanopartículas multifuncionais para a entrega intracelular de um anticorpo a células cancerígenas com expressão de CD44v6

Multifunctional nanomedicine for the intracellular delivery of an antibody to CD44v6 expressing cancer cells

Universidade de Aveiro
2019

Departamento de Ciências Médicas

ANA ISABEL BAIÃO VIEIRA

Nanopartículas multifuncionais para a entrega intracelular de um anticorpo a células cancerígenas com expressão de CD44v6

Multifunctional nanomedicine for the intracellular delivery of an antibody to CD44v6 expressing cancer cells

Dissertação apresentada à Universidade de Aveiro para cumprimento dos requisitos necessários à obtenção do grau de Mestre em Biomedicina Molecular, realizada sob a orientação da Professora Doutora Odete Abreu Beirão da Cruz e Silva, Professora Associada com Agregação do Departamento de Ciências Médicas da Universidade de Aveiro, e co-orientação científica do Professor Doutor Bruno Filipe Carmelino Cardoso Sarmento, Investigador Principal do Grupo *Nanomedicines & Translational Drug Delivery* do Instituto Nacional de Engenharia Biomédica/Instituto de Investigação e Inovação em Saúde – Universidade do Porto.

Apoio financeiro do Fundo Europeu de Desenvolvimento Regional (FEDER), através dos programas NORTE 2020 e COMPETE 2020, e da FCT – Fundação para a Ciência e a Tecnologia.

Dedico este trabalho aos meus pais.

o júri

presidente

Professor Doutor Ramiro Daniel Carvalho de Almeida
Professor Auxiliar do Departamento de Ciências Médicas da Universidade de Aveiro

Doutora Catarina da Costa Moura
Investigadora do Departamento de Ciências da Vida do Laboratório Ibérico Internacional de Nanotecnologia

Professor Doutor Bruno Filipe Carmelino Cardoso Sarmento
Investigador Principal do Instituto Nacional de Engenharia Biomédica/Instituto de Investigação e Inovação em Saúde da Universidade do Porto

agradecimentos

Em primeiro lugar, quero agradecer ao Doutor Bruno Sarmento por me dar a oportunidade de desenvolver a dissertação de mestrado no grupo *Nanomedicines & Translational Drug Delivery* do INEB/i3S. Obrigada por toda a disponibilidade e orientação ao longo do último ano, e por todo o conhecimento partilhado.

À Doutora Odete Silva pela disponibilidade e orientação.

À Doutora Carla Oliveira quero agradecer por estar disponível para me fornecer as linhas celulares usadas, essenciais para o desenvolvimento desta dissertação.

A todos os membros do grupo de investigação, um agradecimento enorme por me terem ensinado tanto e por estarem sempre disponíveis para me ajudar em todas as situações. Ao Patrick por me ter guiado no início do trabalho e por todas as sugestões tão importante para quem estava a começar. À Vanessa por ter sido a minha mentora na fase inicial do trabalho, por ouvir sempre as minhas preocupações e por tirar sempre a parte positiva das situações menos boas. À Flávia, por toda a ajuda na fase mais final do trabalho, pela disponibilidade e por todas as dicas. Obrigada por todo o apoio.

Aos meus amigos. À Patrícia por ter partilhado comigo este desafio como colega de instituto e colega de casa, por todos os momentos de conversa e por ter estado sempre disponível. À Rafaela, por todo o apoio ao longo deste ano e por estar sempre pronta para me ajudar. À Andreia, por ter sido a minha companheira de mestrado e por todos os bons e maus momentos partilhados. Aos Miguitos, obrigada por tudo ao longo destes anos, por estarem sempre do meu lado e por ouvirem os meus dilemas nos cafés de fim de semana.

Ao Zé, por toda a paciência, compreensão e apoio incansável.

Por fim e mais importante, obrigada à minha família. Aos meus padrinhos por todo o carinho. Aos meus pais e à minha irmã obrigada por todo o esforço e sacrifício. Obrigada por serem o meu maior pilar, por acreditarem sempre em mim e por todo o apoio incondicional. Obrigada por tudo.

palavras-chave

Bevacizumab, cancro colorretal metastático, CD44v6, fragmento de anticorpo, nanopartículas de PLGA-PEG

resumo

O cancro colorretal (CCR) é um dos cancros mais incidentes e mortais no mundo, maioritariamente devido à sua capacidade de metastização. A isoforma do recetor CD44 com o exão 6 (CD44v6) nas células colorretais tem sido envolvida em diversos processos cancerígenos, incluindo metástases. O CD44v6 é coreceptor para o fator de crescimento de hepatócitos (HGF) e fator de crescimento endotelial vascular (VEGF), junto com o c-Met e o recetor VEGF 2 (VEGFR-2), respetivamente. Os regimes padrão de quimioterapia recomendada para os estádios metastáticos do CCR estão frequentemente associados a efeitos secundários graves, uma vez que não atuam seletivamente. As terapias que atuam seletivamente contra um alvo molecular melhoram a eficácia dos fármacos, resultando em menor toxicidade. Um exemplo é o bevacizumab (Avastin®), um anticorpo monoclonal (mAb) que atua inibindo a ação do VEGF. Sistemas de entrega de fármacos (DDS), como nanopartículas (NPs), podem ser conjugados com ligandos de modo a serem direcionados para um alvo molecular específico. Um tipo de ligando com elevada afinidade para recetores celulares são os anticorpos. Neste trabalho foi desenvolvido um nanosistema inovador, com NPs poliméricas de poli(ácido láctico-co-glicólico)-polietilenoglicol (PLGA-PEG) encapsuladas com bevacizumab e conjugadas com um fragmento de anticorpo (Fab) específico para células cancerígenas humanas com expressão de CD44v6, o AbD15179 (Fab v6). Foram também produzidas NPs não funcionalizadas e com um Fab (-) para avaliar a especificidade do Fab v6. As NPs produzidas apresentaram um tamanho entre 200 a 300 nm e uma carga elétrica superficial negativa entre -5 e -10 mV, com uma eficiência de associação (EA) do bevacizumab de cerca de 85%. No geral, as formulações com uma concentração de 5 e 50 µg/mL não demonstraram toxicidade em células cancerígenas. As NPs de PLGA-PEG Fab v6 ligaram-se especificamente à superfície das células que sobreexpressam o CD44v6 e essa afinidade foi mantida com a encapsulação de bevacizumab. Além disso, as NPs PLGA-PEG Fab v6 mostraram maior internalização celular do que as NPs não funcionalizadas e Fab (-). De modo a confirmar a especificidade das NPs PLGA-PEG Fab v6 com bevacizumab, os níveis intracelulares de bevacizumab e VEGF foram avaliados. Os níveis intracelulares de bevacizumab foram significativamente mais elevados nas células incubadas com NPs PLGA-PEG Fab v6. Os níveis intracelulares de VEGF não mostraram significância entre os grupos, mas foi possível observar uma tendência na diminuição dos níveis de VEGF após a incubação das NPs PLGA-PEG Fab v6. Neste trabalho foi demonstrado que é possível encapsular um mAb em NPs PLGA-PEG e funcionalizar com um Fab para uma entrega intracelular do fármaco específica efetiva. No entanto, o seu uso na entrega de fármacos requer mais investigação e otimização.

keywords

Antibody fragment, bevacizumab, CD44v6, metastatic colorectal cancer, PLGA-PEG nanoparticles

abstract

Colorectal cancer (CRC) is one of the most incident and mortal cancers in the world, mainly due to its metastatic ability. CD44 receptor isoform containing exon 6 (CD44v6) in colorectal cells have been implied in many cancers associated process including metastasis. CD44v6 is a co-receptor for hepatocyte growth factor (HGF) and vascular endothelial growth factor (VEGF), along with c-Met and VEGF receptor 2 (VEGFR-2), respectively. Standard chemotherapy regimens recommend for metastatic stages of CRC are commonly associated with severe side effects because they act non-selectively. Therapies that act specifically against a molecular target enhance efficacy of the drugs, resulting in lower toxicity. One example is bevacizumab (Avastin®), an anti-angiogenic monoclonal antibody (mAb) that inhibits VEGF action. Drug delivery systems (DDS), as nanoparticles (NPs) can be conjugated with ligands in order to be directed to a specific molecular target. One type of ligand with high affinity to cell receptors are antibodies. In this work, it was developed an innovate nanosystem, with polymeric NPs of poly(lactic-co-glycolic acid)-polyethylene glycol (PLGA-PEG) loaded with bevacizumab and decorated with an antibody fragment (Fab) specific for CD44v6-expressing human cancer cells, the AbD15179 (v6 Fab). Bare and (-) Fab PLGA-PEG NPs were also developed to evaluate the specificity of v6 Fab. The NPs produced displayed sizes in the range of 200-300 nm and a negative surface electric charge between -5 and -10 mV, with an association efficiency (AE) of bevacizumab around 85%. Overall, the formulations at a concentration of 5 and 50 µg/mL did not show toxicity in cancer cells. The v6 Fab-PLGA-PEG NPs specifically bonded to the surface of cells overexpressing CD44v6 and this affinity was maintained with the encapsulation of bevacizumab. Also, PLGA-PEG NPs functionalized with v6 Fab were more internalized in cells than the bare and (-) Fab-PLGA-PEG NPs. To confirm the specificity of bevacizumab-loaded v6Fab-PLGA-PEG NPs, intracellular levels of bevacizumab and VEGF were evaluated after incubation of PLGA-PEG NPs. Intracellular levels of bevacizumab were significantly higher in cells incubated with v6 Fab-PLGA-PEG NPs. The percentage of intracellular VEGF levels did not show significance between the groups but was possible to observe a tendency in the decrease of VEGF levels after incubation with v6 Fab-PLGA-PEG NPs. In this work it was demonstrated that it is possible to encapsulate a mAb in PLGA-PEG NPs and then functionalize with a Fab for a specific and effective intracellular delivery of the drug. Though, their use in drug delivery requires further investigation and optimization.

List of contents

List of Figures

List of Tables

Acronyms and Abbreviations

A

AbD15179	Human, anti-human CD44v6 Fab
ADCC	Antibody-dependent cellular cytotoxicity
AE	Association efficiency
AJCC	American Joint Cancer Committee
Akt	Protein kinase B
APC	Allophycocyanin

B

BSA	Bovine serum albumin

C

CAF	Cancer associated fibroblasts
CAM	Cell adhesion molecule
CD44	Cluster of differentiation 44
CD44std	Standard isoform of CD44
CD44v	Variant isoform of CD44
CD44v6	Variant isoforms of CD44 containing exon v6
CDC	Complement-dependent cytotoxicity
CDR	Complementarity-determining region
CH	Constant region of the heavy chain
CIN	Chromosomal instability
CIM	CpG island methylator phenotype
CL	Constant region of the light chain
CRC	Colorectal cancer

CR-CSC	Colorectal cancer stem cells
CSC	Cancer stem cell
CpG	Dinucleotide cytosine-guanine

D

DDS	Drug delivery system
DL	Drug loading
DLS	Dynamic light scattering
DMSO	Dimethyl sulfoxide
Dox	Doxorubicin
DTX	Docetaxel

E

EA	Ethyl acetate
ECM	Extracellular matrix
EGF	Epidermal growth factor
ELISA	Enzyme-linked immunosorbent assay
ELS	Electrophoretic light scattering
EMA	European Medicines Agency
EMT	Epithelial-to-mesenchymal transition
EPR	Enhanced permeation and retention
ERM	Ezrin, radixin, moesin

F

Fab	Fragment antigen binding
FACS	Fluorescence-activated cell sorting
FBS	Fetal bovine serum

Fc	Fragment crystallizable region
FcR	Fragment crystallizable region receptor
FDA	Food and drug administration
FKR648	Fluorescent dye with emission at 648 nm
Fv	Fragment variable region

G

GBM	Glioblastoma
GFP	Green fluorescent protein

H

HA	Hyaluronic acid
HER	Human epidermal growth factor receptor
HGF	Hepatocyte growth factor
HIF	Hypoxia-inducible factor
HNSCC	Head and neck squamous cell carcinoma
HPLC	High pressure liquid chromatography
HRP	Horse radish peroxidase
HuCAL	Human combinatorial antibody library

I

Ig	Immunoglobulin
IgG	Immunoglobulin G
IL-6	Interleukin 6

J

JCRB	Japanese Collection of Research Bioresources

M

mAb	Monoclonal antibody
Mal	Maleimide
MAPK	Mitogen activated protein kinase
mCRC	Metastatic colorectal cancer
MDR	Multiple drug resistance
MET	Mesenchymal-epithelial transition
MFI	Mean fluorescence intensity
MSI-H	High microsatellite instability
MTT	3-(4,5-dimethylthiazol-2-yl)-2,5-diphenyltetrazolium bromide

N

NHS	*N*-hydrosuccinimide
NK	Natural killer
NPs	Nanoparticles

O

OPN	Osteopontin

P

PBS	Phosphate buffered solution
PBST	PBS containing 0.1% Tween-20
PdI	Polydispersity index
PE	Phycoerythrin
PEG	Polyethylene glycol
PFA	Paraformaldehyde
PI3K	Phosphoinositide 3-kinase

PLA	Poly(lactic acid)
PLGA	Poly(lactic-co-glycolic acid)
PMA	Phorbol 12-myristate 13-acetate
PMSA	Prostate-specific membrane antigen
PTX	Paclitaxel

R

RES	Reticulo-endothelial system
RPMI	Roswell park memorial institute
RP-HPLC	Reversed-phase high pressure liquid chromatography
RT	Room temperature

S

scFv	Single-chain variable fragment
sdAb	Single-domain antibody
SDF-1	Stromal cell-derived factor 1
SLN	Solid lipid nanoparticles

T

T/E	Trypsin/EDTA
TCEP	Tris(2-carboxyethyl) phosphine
TEM	Transmission electron microscopy
TFA	Trifluoroacetic acid
TGF-β1	Transforming growth factor β1
TMB	3,3′,5,5′-Tetramethylbenzidine

U

UICC	Union for International Cancer Control

V

VEGF	Vascular endothelial growth factor
VEGFR	Vascular endothelial growth factor receptor
VH	Variable domain from the heavy chain
VL	Variable domain from the light chain

W

w/o/w	Water-in-oil-in-water

Chapter I – Introduction

1. Colorectal Cancer

1.1. Physiopathology of Colorectal Cancer

Colorectal cancer (CRC) is the 3rd most incident cancer and the 2nd most deadly cancer worldwide [1]. CRC manifests through the accumulation of genetic modifications that are responsible to change the normal epithelium to adenomatous lesions, developing carcinoma [2, 3]. Genetic susceptibility plays a role in up to 35% of all CRCs [4]. The molecular pathogenesis of CRC is heterogeneous and could follow three different molecular mechanisms [5, 6], namely: i) chromosomal instability (CIN), ii) high microsatellite instability (MSI-H), or iii) CpG island methylator phenotype (CIMP). CIN mechanism is the cause of more than 70% of sporadic CRCs and it is the pathway most related with frequent chromosomic modifications [2]. This pathway begins through mutations in adenomatous polyposis coli gene and is further promoted by activating mutations of the *K-Ras* oncogene and inactivating mutations of the *TP53* tumor suppressor gene [3]. CIN tumors are characterized by aneuploidy and loss of heterozygosity. MSI-H pathway contributes for 15% of sporadic CRCs and is characterized by the deficiency on the DNA mismatch repair system [7]. In the mismatch repair-deficient CRCs there is an accumulation of inactivating mutations in repairing genes, such as *hMSH2*, *hMSH3*, *hMLH1*, *hPMS2*, *hPMS1* and *hMLH3*.This phenotype is also characterized by mutation of oncogene *BRAF* and is a hallmark condition in familial Lynch Syndrome. Lastly, CIMP is characterized by the hypermethylation of tumor suppressor genes, most importantly *MGMT* and *MLH1*, leading to their silencing [8]. Almost all cases of tumors with *BRAF* mutations follow this tumorigenesis pathway [9]. Tumors that are considered to belong to MSI-H pathway are frequently associated to methylation of *MLH1* which is associated with CIMP positive tumors. These three pathways of CRC are characterized by an accumulation of genetic alterations and have characteristics that overlap between them.

The progression of CRC occur through the epithelial-mesenchymal transition (EMT), a reversible process characterized by the loss of epithelial properties, including the polarity apico-basal, cell-cell contacts (by E-cadherins) and the overexpression of N-cadherin and fibronectin (i.e. events that favour the cell mobility) (**Figure 1**) [10]. Also, presence of nuclear β-catenin is correlated with the induction of EMT. A series of transcription factors, as Snail,

Twist and Zeb, are undergoing EMT, regulated by a combination of extracellular signals [11]. These signals can be activated during cancer progression by the receptor tyrosine kinase c-Met pathway. The c-Met and its cognate high-affinity ligand hepatocyte growth factor (HGF), control invasive growth through the coordination of cell proliferation, survival, EMT and migration/invasion. After cells intravasate into lymph and blood vessels, solitary carcinoma cells can extravasate and remain solitary, forming a micrometastasis, or they can form a macrometastasis through the reversible process of EMT, the mesenchymal-epithelial transition (MET) [12].

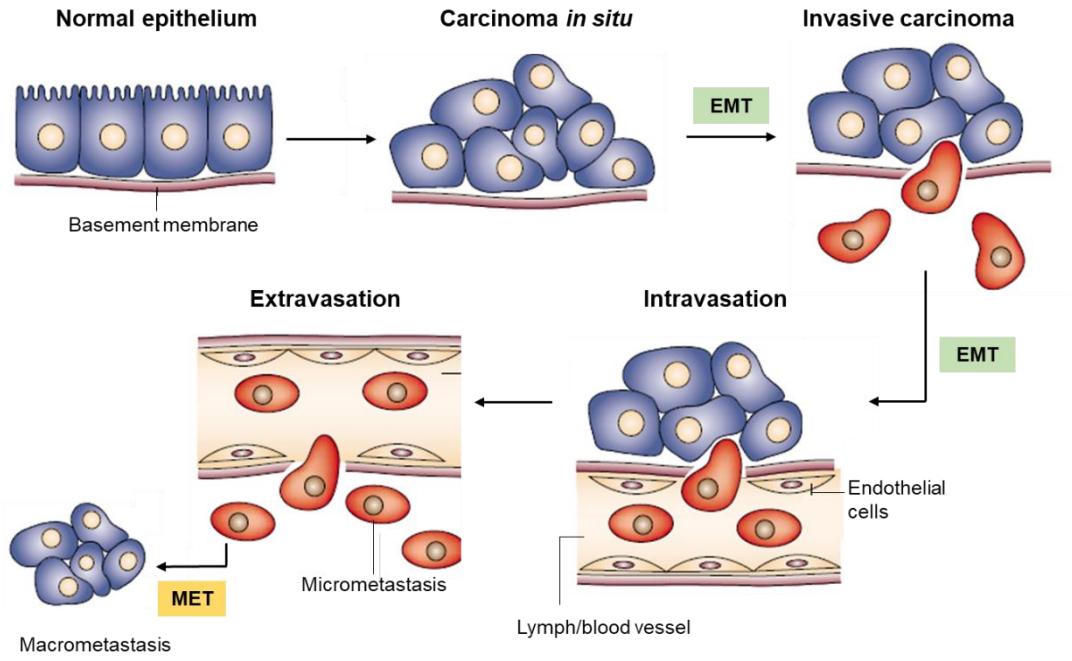

Figure 1. EMT and MET on progression of tumor. Normal epithelium can proliferate locally and be altered by epigenetic and genetic changes leading to a carcinoma *in situ*. Further alterations can induce the disruption of basement membrane and the local dissemination of the cells, through an epithelial-mesenchymal transition (EMT). The cells can intravasate into lymph or blood vessels, being transported passively to distant organs. When in secondary locations, the carcinoma cells can extravasate and form a micrometastasis, or they can form a new carcinoma by mesenchymal-epithelial transition (MET). Adapted from [12].

It is well-known that metastatic dissemination is present in about 50% of patients with CRCs [13], with a frequency of 30-70% in liver, 20-40% into the lung and 5-10% into the bone and lower frequencies into brain, adrenal gland and ovary [14]. Metastatic colorectal cancers (mCRC) are characterized by cells with capacity of invasion, deregulated adhesion, resistance to apoptosis and ability to modulate the environment.

Another characteristic of CRC pathology is related with cancer stem cells (CSCs). CSCs are a set of cells in a tumor that have the capacity to generate differentiated cells from a small sub-group of undifferentiated cells, which are also capable of self-renewal [15]. Several cellular markers of CRC, such CD44, CD133, CD166 and EpCAM are able to identify CSCs [16].

According to the American Joint Cancer Committee (AJCC)/Union for International Cancer Control (UICC) TNM classification, 7th edition, the pathological stage of the cancer is classified by the invasion of primary tumor (T stage), lymph node involvement (N stage), and presence of distant metastases (M stage). These stages are important because they provide the basis for therapeutic decisions, being crucial for the disease prognosis [17].

1.2. Colorectal Cancer Therapies

The treatment of CRC is defined according to several factors, such as location, size and the extent of cancer spreading [18]. It includes surgery, radiofrequency ablation, cryosurgery, radiotherapy and chemotherapy. An important first line of defence against cancer is surgery and is the base treatment for the patients in stages of primary tumor (stages I and II) [19]. In patients in a more advanced stage of cancer (stage III), where surgical resection has already been done, adjuvant chemotherapy is recommended [17, 20]. Patients in stage IV (distant metastasis) with resectable metastasis should be indicated for surgical resection of the metastasis. In patients with irresectable metastasis, the management consists of palliative chemotherapy.

The current treatment of CRC is based on four chemotherapeutic drugs, 5-fluorouracile (5-FU), oxaliplatin, irinotecan and leucovorin [6]. The first-line chemotherapy comprises a fluoropyrimidine (intravenous 5-FU or oral capecitabine) used in different combinations with oxaliplatin, irinotecan and leucovorin [21]. Combination treatments of these drugs include 5-FU/leucovorin with oxaliplatin (FOLFOX4), 5-FU/leucovorin with irinotecan (FOLFIRI), 5-FU/leucovorin, and oxaliplatin and irinotecan (FOLFIRINOX). When the first-line strategy of therapy fails, the chemotherapy backbone should be changed, and a second-line therapy is proposed. Therapies that act selectively against molecular targets involved in the growth, progression and spread of cancer cells have been developed [6]. Drugs that have as targets vascular endothelial growth factor (VEGF) and epidermal growth factor (EGF) receptors have improved outcomes in the chemotherapeutic treatment of mCRC [5, 22]. Cetuximab (Erbitux®) and panitumumab (Vectibix®) are two humanized monoclonal antibodies (mAbs) that inhibit the activation of EGF receptors (EGFR). Studies

have been showed a reduced risk of progression of *KRAS* wild-type mCRC when cetuximab or panitumumab was added to the first-line treatment regime FOLFIRI [23, 24]. Also, mAbs as antiangiogenic agents, such as bevacizumab (Avastin®) and ramucirumab (Cyramza®), have been used to target VEGF and VEGF receptor 2 (VEGFR-2), respectively. Bevacizumab has been introduced for first- and second-line treatment of mCRC, in combination with intravenous 5-FU-based chemotherapy, improving the overall survival of the patients [25-27].

Nevertheless, therapies acting non-selectively, namely the drugs used in first-line therapy, are frequently associated with common and major side effects [6]. Therapies that do not act against specifically a molecular target act also against healthy tissues and cells, being associated with a high toxicity profile [28, 29]. Also, the mortality rates still remain high due to the development of chemotherapy resistance.

2. CD44v6 as a Target for Colorectal Cancer Directed Therapies

2.1. CD44 General Biology and Structure of its Isoforms

Cluster of differentiation 44 (CD44) forms a family of multifunctional, single-chain transmembrane glycoproteins belonging to the class of cell adhesion molecules (CAMs) [30]. Selectins, integrins and cadherins belong to the CAMs family that control cell behaviour by mediating cell-cell and cell-matrix contact, cell growth and trafficking, EMT and tumor progression [31]. CD44 is consequently essential for maintaining tissue integrity [32]. CD44 is accepted as a biomarker for CSCs, tumor initiating potential and invasiveness of cancer cells [33, 34]. CD44 major ligand is hyaluronic acid (HA), the most abundant component of extracellular matrix (ECM). However, CD44 also has binding sites for collagen, laminin, fibronectin and many others [33]. All the isoforms belonging to this family of proteins are encoded by a single gene present on chromosome 11 in humans. *CD44* gene has seven extracellular domains, a transmembrane domain and a cytoplasmatic domain and is composed of 20 exons (10 constant and 10 variable exons. Standard isoform of CD44 (CD44std) is composed of 10 exons (s1-s10) and variant isoforms of CD44 (CD44v) express one or more additional exons between v1-v10 [31]. The heterogeneity of the CD44 family is increased by several posttranslational modifications [30], as differential glycosylation (*N*-glycosylation and *O*-glycosylation) and the insertion of alternatively spliced exon products in the extracellular domains of the molecule [33].

CD44s is present on the membrane of most vertebrate cells and has been more extensively studied as a receptor for HA [33]. CD44v is expressed mainly in epithelial cells being present in several types of carcinoma and in some cases play a well-defined role, depending on which tissue it is expressed [30]. In many cancers, the expression of CDD4s and CD44v isoforms correlates with advanced stages of carcinogenesis [35]. Among CD44v isoforms, CD44v containing exon 6 (CD44v6) seems to play a major role in cancer progression [30]. Its expression correlates with poor prognosis, metastatic potential and aggressive stages of CRCs [36].

2.2. CD44v6 Biology

CD44v6 became object of clinical interest after Gunthert *et al.* showed that overexpression of CD44v6 in rat pancreatic cancer cells confers metastatic capacity [37]. This initial study of CD44v6 biology and its potential as a therapeutic target and prognostic marker started several studies to discover all the characteristics of CD44v6 and its relevance in cancer therapy.

CD44v6 is mainly expressed in proliferative tissues, including the skin [38] and the crypts of the intestine [36] but is also found in the endothelium and activated lymphocytes. CD44v6-containing isoforms have been shown to play a prominent role in the establishment of primary tumors [32] as well in metastasis [37]. CD44v6 contains a binding site for HGF, VEGF [33], osteopontin (OPN), and other major cytokines produced by tumor environment that can cause increased CD44v6 expression in colorectal cancer stem cells (CR-CSCs) [39].

CD44v6 participates in the HGF-mediated activation [39] and internalization of the HGF receptor c-Met [40] that is predominantly expressed in epithelial cells (**Figure 2**) [41]. CD44v6 isoforms also play a dual role for c-Met-dependent signalling. The extracellular domain of CD44v6 is required for c-Met activation [32], whereas the cytoplasmatic domain recruit ERM proteins (Ezrin-Radixin-Moesin) that bind the cytoskeleton in order to promote activation of Ras/MAPK pathway. Also, other signalling pathways starting at the c-Met receptor, as PI3K-Akt pathway, depend on the function of the CD44v6 cytoplasmatic tail [42]. Ras signalling promotes CD44v6 alternative signalling that sustains late Ras signalling, creating a positive feedback loop which has shown to be important for cell cycle progression [43].

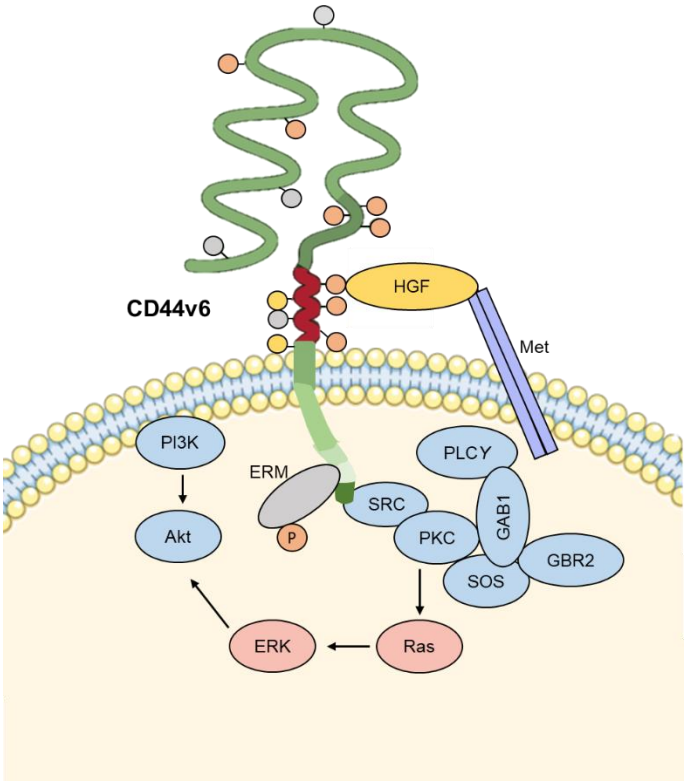

Figure 2. Regulation of Met by CD44v6. Extracellular domain of CD44v6 binds HGF and presents it to Met, which is activated. The downstream signalling cascades require activation of CD44-associated ERM proteins through the cytoplasmatic tail of CD44v6. Activation of Ras/MAPK and PI3K/Akt pathways is important for cell proliferation. Adapted from [33].

CD44v6 co-receptor function is not restricted to epithelial cells, it can control endothelial cell migration, sprouting, and tubule formation induced by HGF or VEGF-A. HGF and VEGF are two potent angiogenic factors [44] which are interrelated once the expression of HGF and its receptor c-Met correlates with tumor vascularization, and HGF induce and potentiate the activity of VEGF. The most prominent receptor tyrosine kinase involved in angiogenesis, the VEGFR-2, is also dependent-regulated by CD44v6 [45] in a manner that is similar to that described for Met. CD44v6 and VEGFR-2 are constitutively associated [35], in contrast to Met, which needs its HGF ligand to interact with CD44v6 [41].

2.3. CD44v6 in Cancer

Da Cunha *et al.* described for the first time the overexpression of CD44v6 in hyperplasic lesions of the gastric mucosa, which is directly correlated to the severity of cancer [46]. This study also found that overexpression of CD44v6 is associated with a diminished/abnormal expression of E-cadherin. E-cadherin has an important role in cancers

[47] and its loss of expression is related to EMT, an important process on development of metastasis [12]. Cancer cells increase self-renewal and migration through EMT favouring the appearance of CSCs. Microenvironmental signals were found to increase EMT and metastatic potential of CR-CSCs promoting the expression of CD44v6, which acts as both functional biomarker and therapeutic target. This study demonstrated that the metastatic process in CRC is initiated by CSC through the expression of CD44v6 in CR-CSCs [39]. In this way, CD44v6 is a marker predictor for metastasis in CR-CSCs and its expression is increased by cytokines, HGF, OPN, stromal cell-derived factor 1 (SDF-1) secreted from tumor-associated cells such cancer-associated fibroblasts (CAFs). These compounds provide metastatic activity to tumorigenic cells.

The first therapeutic developed directed against CD44v6 was the mAb bivatuzumab [48]. Clinical trials were conducted in patients with histologically confirmed squamous cell carcinoma of the head and neck or oesophagus. Although it seems that the antibody had targeted the tumor with success in some of the patients, many of them developed serious adverse effects and one patient developed toxic epidermal necrolysis leading to death [48]. The use of this targeted drug in clinic was abolished due the toxicity effects.

The use of mAbs directed towards specific CD44v6 epitopes inhibited the activation of c-Met by HGF [41] through a mutation on three specific residues of the v6 exon [49]. Following this work, it was possible the production of a peptide with five amino acid containing these three specific residues to disrupt the activation of c-Met. This peptide also inhibits VEGFR-2 binding [45], blocking angiogenesis, and showed the inhibition of tumor growth and metastasis in pancreatic cancer models [50].

A fragment antigen binding (Fab) with specificity for CD44v6 was developed from a chimeric mAb and tested on CD44v6-expressing head and neck squamous cell carcinoma (HNSCC) cells [51]. The study showed that the conjugate was stable and had affinity to CD44v6. Also, a biodistribution study was performed and the fragment demonstrated better tumor penetration and a superior tumor-to-blood ratio. AbD15179 is a CD44v6-targeting antibody fragment selected and screened from HuCAL (human combinatorial antibody library) PLATINUM library [52, 53]. The specificity of AbD15179 for CD44v6 expressing cells has been confirmed in the last years. Radiolabelled AbD15179 displayed high and specific tumor uptake in CD44v6-expressing squamous cell carcinoma xenografts [54] and improved avidity and slower dissociation rate [55]. A study with nanoparticles (NPs) also showed the specificity of AbD15179 for CD44v6 receptor [56]. In this study, PLGA-PEG

NPs were functionalized at the surface with AbD15179 and specifically bound to intestinal-type cells overexpressing CD44v6.

CD44v6 is a suitable target for drug delivery and/or immunodiagnostics and AbD15179 fragment can improve targeted therapy directed to CD44v6 overexpressed in CRC cells but can also to other diseases that have CD44v6 abnormal expression.

3. Nanoparticles for Targeted Drug Delivery

3.1. The Beginning of Nanomedicine

Nanotechnology is a complex area involving different fields, such chemistry, biology, applied physics, optics and materials science. Nanotechnology allows a nanosystems production to diagnose, as accurately and early as possible, and treat, as effectively as possible, a disease, avoiding the side effects of free drugs and resulting in health benefits.

Treatment of cancer have as standard therapy chemotherapy, radiotherapy and surgery resection. However, conventional cancer therapies usually cause cytotoxicity resulting in severe side effects since they do not distinguish healthy cells from cancer cells. Nanotechnology as drug delivery systems (DDS) has the ability to improve the drug therapeutic index by increasing efficacy and/or reducing the toxicity effects [57]. The incorporation of therapeutic molecules into nanocarriers might enhance the pharmacological properties of drug, such as stability, solubility, circulating half-lime and tumor accumulation [58]. This is due to the facility of nanosystem to control the drug release rate and to deliver a molecular drug to intracellular sites of action. However, besides drug delivery, nanotechnology can be also used to develop more sensitive systems for cancer diagnosis and imaging [59, 60]. Therapeutic nanocarriers as NPs for cancer treatment are mainly administrated systemically and accumulated in tumor by the enhanced permeability and retention (EPR) effect [28]. In EPR effect, NPs escape into the tumor tissues due to increased permeability of the blood vessels and the dysfunctional lymphatic drainage, two general features of tumors [61]. The systemic delivery of NPs is a complex process in which multiple biological effects can affect the effect of the drug, such as blood circulation, extravasation and interaction with tumor environment, tumor tissue penetration and cell internalization. The characteristics of NPs influence these biological processes, thus being determinant factors for the therapeutic outcome of the drug.

3.2. Types of Nanosystems

There are currently different types of nanocarriers that can be divide into organic (liposomes, polymeric micelles, polymeric NPs and dendrimers), inorganic (iron oxide NPs, gold NPs, mesoporous silica NPs, carbon NPs and quantum dots), and hybrid organic-inorganic particles [62]. Relatively to the NPs formulations, the most commonly explored material are polymers and they can be classified as synthetic (e.g. poly(lactic acid) (PLA) or poly(lactic co-glycolic acid (PLGA)) or natural (e.g. chitosan and collagen) [63]. Polymeric NPs have shown advantages relative to other materials [64]. They have the ability to encapsulate drugs into their cores, as opposed to surface attachment, protecting their cargo from degradation and improving the bioavailability of the drug and their retention time. The encapsulation of a drug into polymeric NPs increase drug efficacy, specificity and tolerability, reducing the risks to patients. PLGA is one of the most used polymers due its advantageous features in drug delivery [65]. It is biodegradable, biocompatible and is associated with a minimal systemic toxicity, being approved by the Food and Drug Administration (FDA) and European Medicine Agency (EMA) [66]. Also, PLGA NPs have the versatility to encapsulate either hydrophobic or hydrophilic drugs.

PLGA NPs are internalized in cells mainly by endocytosis [67]. As PLGA is a hydrophobic material, the body recognizes PLGA NPs as a foreign body and the reticulo-endothelial system (RES) eliminating these from the blood stream, being retained in the liver or the spleen. These biological barrier for DDS can be overcome by surface modification of NPs [68]. NPs can be coated with molecules that hide the hydrophobicity and make them invisible to the RES. Polyethylene glycol (PEG) is a hydrophilic polymer and it is the most common moiety used for surface modification [69]. Coating NPs surface with PEG block electrostatic and hydrophobic interactions, increasing their blood circulation half-time and therefore increasing specific binding and internalization of NPs into the desired tumors cells or organs [70]. PEG-based polymers can also be used in bioconjugation applications in order to coupling a ligand to the surface of NPs [71].

3.3. Nanomedicines in Cancer

There are already nanocarriers formulations approved clinically and they are used in treatment of different types of cancers with different stages. Doxil® was the first nanomedicine approved by FDA and consists in a pegylated liposome for doxorubicin (dox) encapsulation [72]. It was approved for the treatment of HIV-related Kaposi's sarcoma, metastatic ovarian cancer and metastatic breast cancer. Since then, other cancer

nanomedicines have reached the market and others are in different phases of clinical trials [73]. DDS approved by FDA include liposome, polymer, micelle, nanocrystal, inorganic and protein NPs [74] and have indications for different diseases, besides cancer. For the treatment of cancer, stand out the liposome, polymer and protein NPs. Between approved liposomes, Marqibo® [75] and Vyxeos™ [76] are indicated for leukaemia and Onivyde® for pancreatic cancer [77]. Eligard® [78] and Oncaspar® [79] are polymeric NPs approved for the treatment of prostate cancer and acute lymphoblastic leukaemia, respectively. There are also other nanoformulations approved by EMA such MEPACT® (liposomal mifamurtide) [80] and Myocet™ (non-PEGylated liposomal dox) [81].

NPs for the treatment of CRC are normally loaded with drugs used in conventional chemotherapies (e.g. 5-FU, irinotecan) or targeted drug as cetuximab and rapamycin. Liposomes are the most well stablished nanocarriers and some are currently under clinical study for the treatment of CRC [73]. Examples are CPX-1 (loaded with irinotecan/floxuridine) that completed phase II of clinical trials [82], and Thermadox® (dox) [83]. Also, several agents have shown promising *in vitro* results including oxaliplatin-loaded long circulating liposomes, liposomal curcumin and dox-encapsulated liposome.

However, polymer NPs are considered more stable than liposomes and several formulations for CRC therapy have shown a good pharmacokinetic performance [73]. NK911 and SP1049C, two polymeric formulations loaded with dox, are produced with a copolymer of PEG plus dox-conjugated poly(aspartic acid) and pluronic micelles, respectively, and have shown better results in tumors in comparison with drug alone [84]. NK105 is a polymeric micelle loaded with paclitaxel (PTX) that also showed a better pharmacokinetic profile than PTX alone [85]. However, these formulations did not reach the target directly and the drugs were released into the extracellular matrix, compromising the effectiveness of the drug. In the last years, NPs that have site-specific targeted are a promising advancement in cancer therapy [86]. An example is abraxane, an albumin-based NP formulation that was approved by FDA in 2005 for treatment of metastatic breast cancer and represents a promising advance in the field of targeted nanomedicine [57]. This formulation is PTX-loaded conjugated with albumin molecules, which enhances the transport of NPs across the vascular endothelial, resulting in 50% greater clinical doses of PTX.

3.4. Targeted Drug Delivery

Combining targeted drug delivery and a controlled drug release system has numerous advantages in chemotherapy [87, 88]. Using targeted systems, it is possible concentrate the drug activity on action site reducing its exposure to the healthy tissues and cells. DDS can be conjugated with ligands in order to produce targeted nanosystems able to drive the drug to the specific site of action, increasing the payload of the drug with minimal activity loss and reduced toxicity.

NPs can achieve tumor by active or passive targeting [68]. Passive DDS exploit the characteristics of tumor biology and nanocarriers accumulate in the tumor through EPR effect (**Figure 3**). In this way, retained nanocarriers will release encapsulated drug into the tumor cells. On the other hand, in active targeting, ligands are linked at the NPs surface in order to target a specific cell. The ligand is chosen to specifically bind to overexpressed molecules on the tumor cell surface or tumor vasculature, and not expressed on healthy cells [69, 89]. The interaction between the ligand and the cell receptor allows a specific internalization and the release of the drug inside the cell.

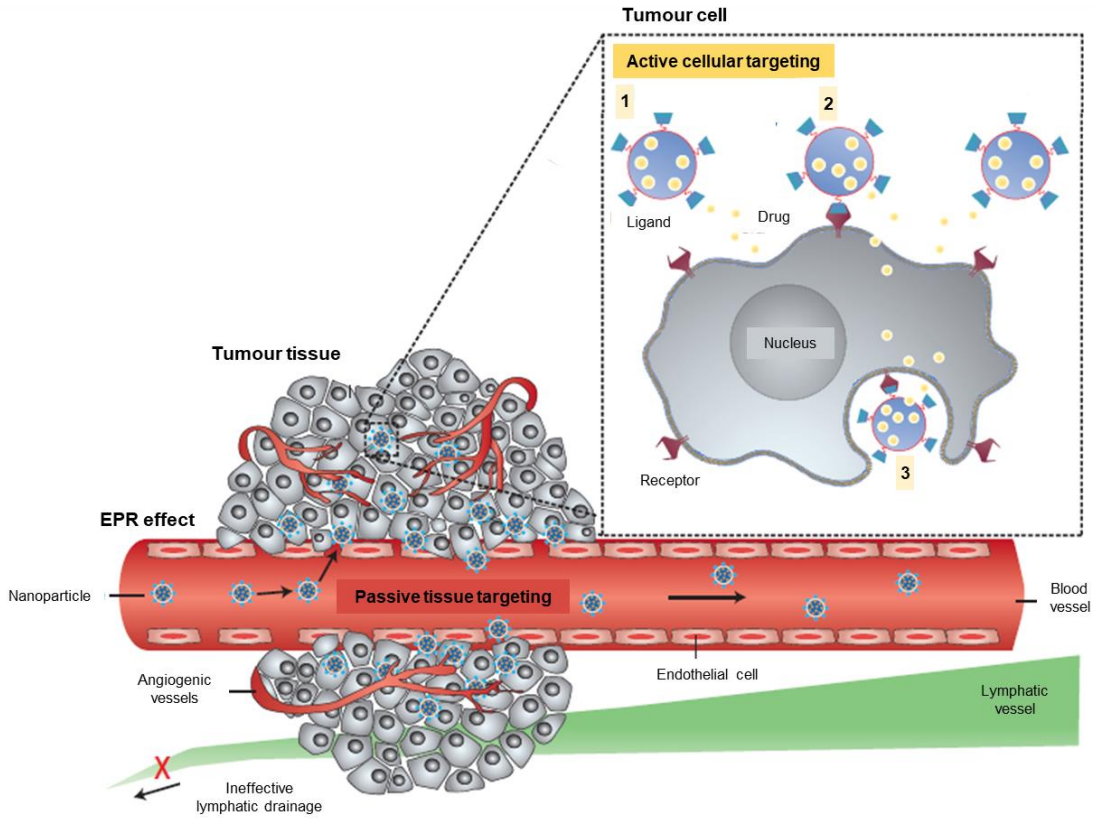

Figure 3. Schematic representation of passive drug delivery (by enhanced permeability and retention (EPR) effect) and active targeted drug delivery to tumors. Adapted from [89].

Passive targeting approach form the basis of clinical therapy but have several limitations. Some drugs are not able to diffuse efficiently, and the approach turns random, which makes difficult to control the targeting. This lack of control may induce multiple drug resistance (MDR), and chemotherapy treatment fail its efficacy due to resistance of cancer cells towards one or more drugs. The passive strategy is further limited because certain tumors do not exhibit the EPR effect, and the permeability of vessels may not be the same throughout a single tumor. Active target can overcome these limitations, programming the nanocarriers so they actively bind to specific cells after extravasation [89].

Conjugated NPs are typically internalized in cells efficiently through an endocytic process [90], which involves NPs invagination on the membrane and then the formation of intracellular vesicles [67]. Once inside the cell, NPs are exposed to the endosome and lysosomal environments and must escape from the lysosomal degradation to reach their intracellular target and release the encapsulated drug [91]. Despite the acidic pH of 5-6 of endosomal and lysosomal compartments, PLGA NPs have the ability to escape to the lysosomal degradation through the selective surface charge reversal of NPs from anionic to cationic [92]. The pH in the endosome increase and eventually, due to the osmotic pressure, the endosome disrupts, and the NPs are released to cytoplasm, in a process called proton sponge effect [93]. Once in cytoplasm, NPs release the drug at a slow rate, resulting in a site-sustained therapeutic effect, which is especially crucial for drugs that require intracellular uptake. Additionally, surface modification of NPs with PEG decrease the clearance of NPs from the bloodstream by the RES [94], increasing significantly the circulation time of the NPs [95].

To develop a targeted therapy, it is necessary to take in account several factors, such as route of administration, biological barriers, adsorption of host proteins to the NP surface, conjugation chemistry, hydrophobicity of NPs, composition, physicochemical characteristics of NP and ligand (size, shape and charge) and the orientation of the conjugated ligand [96].

In general, when using a targeting agent to deliver nanocarriers into cancer cells, it is imperative that the agent binds with high selectivity to molecules that are uniquely expressed on the surface of cancer cells. NPs can be functionalized by conjugating specific units such as proteins (antibodies and their fragments), nucleic acids (in form of DNA or RNA aptamers), or other receptor ligands (peptides, vitamins, carbohydrates), to be able to recognize the target [97].

4. Antibodies in Drug Delivery

4.1. Antibodies as Ligands in Targeted Therapy

mAbs were the first class of targeting molecules and are the most commonly used ligand type to decorate NPs due to their high affinity, specificity, and versatility [98]. To better understand how mAbs can be used as ligands in DDS, it is first necessary introduce antibody biology.

Antibodies or immunoglobulins (Ig) are part of the immune system by recognizing antigens and are secreted by B-cells [99]. Each B lymphocyte clone produces antibodies that are specific for only a single epitope, and in this way, a mAb is an antibody produced by a single clone of B-cells. An antibody is a homodimer composed structurally by two heavy (H) chains (~ 50 kDa each) and two light (L) chains (~ 25 kDa each) and is subdivided into the constant (C) and variable (V) domains, also referred as the Fv region (**Figure 4**) [100]. These chains are linked by disulphide bonds and non-covalent interactions. Each variable domain contains a hypervariable region, the complementary-determining regions (CDRs), that is responsible for the antigen recognition. Antibodies are composed by two identical domains for antigen recognition (Fab) connected with a flexible hinge region to the fragment crystallizable region (Fc) which is involved in effector functions and biodistribution of the antibody [101]. Direct antigen binding to the target is made through CDR of variable domains of Fab and is highly specific. When this binding happens, the constant domain activates the immune effector function mediated by Fc fragment which activates the cells containing Fc receptors (FcR), namely phagocytic cells. The main effector functions of antibodies are opsonisation, classical complement-dependent cytotoxicity (CDC) and natural killer (NK) cell-mediated antibody-dependent cellular cytotoxicity (ADCC) [102].

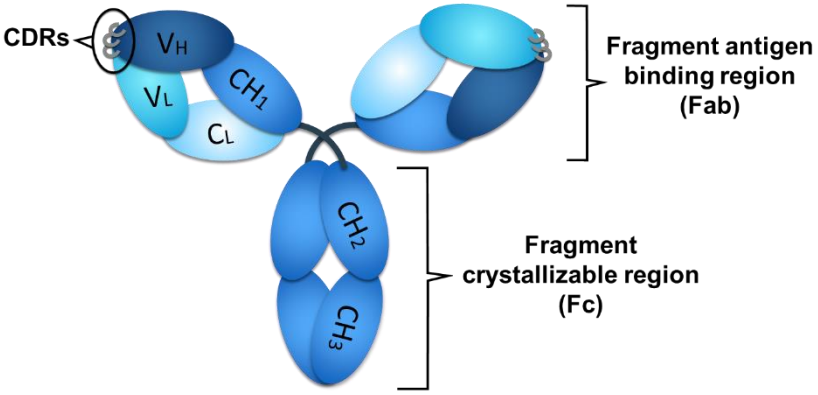

Figure 4. Structure of a whole monoclonal antibody (mAb), include the fragment antigen binding (Fab) and fragment crystallizable (Fc) regions. These regions are composed of the constant (C_H and C_L) and variable (V_H and V_L) domains. The sites for antigen binding are given by complementary-determining regions (CDRs) of the Fab fragment, and immune effector function is mediated by the Fc fragment.

Antibodies are ideal targeting ligands due to their affinity, specificity and engineering malleability [96]. However, the use of the whole antibody has some drawbacks such immunogenicity induction and clearance from bloodstream, due to the binding of FcR to antibody Fc region. Also, the antibody size (~ 150 kDa) difficult cell internalization. To overcome these disadvantages, recombinant techniques have been used to create several different therapeutic antibody formats without loss of full antigen affinity [103] and enable optimize the molecular size, valence, charge and affinity.

The primary building blocks of antibody-based therapy are antibody fragments, namely Fab and single chain Fv (scFv; 25 kDa). The Fabs and the scFv induce less immunogenicity than the whole antibody due to the absence of Fc fragment and retain the affinity and specificity due to the presence of CDRs [97]. Importantly, antibody fragments can be coupled to the surface of NPs in an oriented manner that allow a better recognition of the target. Examples of antibody fragments derivates are Fabs, dimers of antigen-binding fragments ($F(ab')_2$), scFv, single-domain antibodies (sdAbs), among others [62]. Antibody fragments are considered less stable than whole antibodies, however they are considered safer due to reduced non-specific binding [104]. Conjugation of an antibody ligand to the system allows a more selective drug delivery because it enhance the binding of the antibody to their target, with higher affinity.

Nevertheless, ligand orientation on the NPs surface is a critical step for the nanosystem's success. Antibody ligands can be conjugated to NPs by covalent or non-

covalent methods [62]. Non-covalent linkage involves the adsorption of the targeting ligand to the surface of NPs by hydrophobic or electrostatic interactions, for example. With this method the orientation of the ligand is not controlled and their binding to the target is compromised. Also, in these methods can occur the displacement of the absorbed ligand by serum proteins, that can have more affinity for the NPs surface. Ligands covalently linked to the NPs form conjugates more stable and allow a more effective targeting to the receptor. The covalent attachment of targeting ligands at NPs surface can be performed by several chemical methods including carbodiimide chemistry, reactions with *N*-hydrosuccinimide (NHS) active esters, click chemistry reactions such as azide-alkyne cycloaddition and thiol-ene reaction, and the use of thiol reactive groups [105].

In antibody conjugation systems there are two mains chemical reactions that might be applied [106], the carboxyl-to-amine conjugation reaction and the maleimide-to-sulfhydryl conjugation reaction. The carbodiimide chemistry is mainly applied to link with a covalent bond the amine residues (lysine, histidine and arginine) to a structure with a carboxyl group. The maleimide reaction is applied to antibodies that have cysteine residues, once it is the only amino acid that contains a terminal thiol group, necessary to this reaction. This method will be highlighted due to its importance in this work. In maleimide chemistry (**Figure 5**) occurs a reaction between maleimide groups and thiol functions, forming a stable thioether bond.

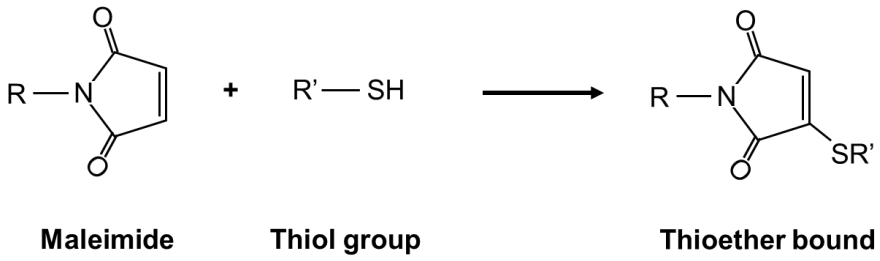

Figure 5. Maleimide-to-sulfhydryl conjugation reaction.

Some proteins present native thiol groups but other thiol functions are absent or present in insufficient quantities [107]. Thus, is necessary to generate sulfhydryl groups (-SH) for the conjugation and it can be done either via heterobifunctional crosslinking agents or by reduction of existing disulphide bonds through reductant agents (such DTT and TCEP). Antibodies molecules contains disulphide groups that bind the two heavy chains and the disulphide bridges between light chain and heavy chain [108]. Selective reduction of some or all of the hinge region disulphides between the two heavy chains can result in a reduced antibody molecule that still maintains its antigen binding capacity.

4.2. Therapeutic Antibodies and Drug Delivery Systems

Recombinant mAbs have been used to treat several diseases, as cancer, asthma and immune and infectious diseases [109]. Their high specificity and affinity allow a targeted therapy, avoiding side effects [110]. Despite the numerous advantages, antibody-based therapy has several limitations [111]. The challenges of antibody-based therapy include the tumor tissue penetration and the mode of action of the drug [112]. The major limitation is attributed to drug distribution, since only a low percentage of administrated dose of mAbs with large size can achieve the tumor [113] and it happens due to “binding site barrier effect”. In “binding site barrier effect”, therapeutic antibodies with high affinity bind their antigen at the periphery of the tumor, and therefore the antibody can only reach the inside of the tumor when the antigens are all saturated on the periphery. It is possible decrease this effect using small antibodies with a low affinity [114].

The majority of human cancers are solid tumors and to the date, of the eight mAbs approved for cancer therapy, only three (trastuzumab, cetuximab, bevacizumab) can be used for this type of tumors [113]. Solid tumors have anatomical and physiological properties that make them hard to penetrate, making a challenge the delivery of effective concentration of the therapeutic antibody [115].

Antibody encapsulation in nanosystems has emerged as an alternative for antibody therapy as it allows to overcome many of the disadvantages and minimize limitations of antibody delivery [116]. The encapsulation of antibodies into nanocarriers reduce unwanted systemic antibody exposure and allow the administration of a lower dose, decreasing toxicity and increasing the patient compliance. Also, allows a sustained antibody release, keeping the plasma concentration of antibodies in a therapeutic range. Furthermore, Srinivasan *et al.* concluded that antibody nanoencapsulation allows an antibody delivery in intracellular components of the cell, for a targeted drug delivery, with lower toxicity [117].

Different types of nanocarriers with mAbs have been developed and NPs for antibody delivery can be produced using biocompatible and biodegradable polymers, lipids or organometallic compounds. Among the different type of polymers, PLGA is the most commonly used polymer in antibody-loaded nanocarriers once it promotes a controlled release of antibodies, allowing a potency enhancement of the therapy [69]. To encapsulate antibodies, the most used method is the modified solvent emulsification-evaporation method based on a water-oil-water (w/o/w) double emulsion technique. In most cases, this technique offers high encapsulation/association efficiency and a controlled release of the antibody. However, nanoencapsulation of antibodies is a critical process once can occur

precipitation and/or aggregation of the antibody that can lead to the instability of antibody and consequent loss of activity [118]. Effects of double emulsion technique on bevacizumab activity were studied by Varshochian *et al.* and concluded that the water/oil interface is the most destabilizing factor. In the formation of the primary emulsion, the antibody tends to migrate to the interface and can lead to its unfolding. The entrapped antibody can potentially interact with the NP matrix and change the antibody structure, which can produce stability issues, loss of bioactivity and increased immunogenicity. In fact, it is necessary assure the stability and bioactivity of antibody when loaded in NPs.

4.3. Bevacizumab

Approximately fifty mAbs are approved by the FDA up to date, since the first mAb was licensed in 1986 [119]. Bevacizumab (Avastin®) is a VEGF-neutralizing mAb and was the first angiogenesis inhibitor to be approved by FDA in 2004 for the treatment of advanced colon cancer [120]. Is now indicated for mCRC, with intravenous 5-FU-based chemotherapy for first- or second-line treatment [121].

Bevacizumab is a humanized immunoglobulin G 1 (IgG1) that binds to human vascular endothelial growth factor A (VEGF-A) and interacts with VEGF receptor tyrosine kinases [122]. VEGF-A is a key regulator of angiogenesis [44] and has a role in the promotion of growth vascular endothelial cells, regulation of vascular permeability and vasodilatation, and induction of endothelial migration [123]. VEGF expression is regulated by hypoxia that increases its transcription by hypoxia-inducible factor 1 (HIF-1). In CRC, interaction of IL-6 with HIF-1 increase the expression of VEGF, contributing for tumor growth. VEGF-A blockade with bevacizumab decreases tumor perfusion, angiogenesis, microvascular density and interstitial fluid pressure in CRCs' patients [124]. Bevacizumab can be used in treatment of several diseases: age-related macular degeneration [125], retinal neovascularization [126], inflammatory diseases of the eye [127], and several cancers, such as cervical cancer [128], mCRC and non-small cell lung carcinoma, among others [102]. Although bevacizumab shows good antiangiogenic activity in some patients, in others the therapy is not effective due to tumor resistance [129]. It is usually administrated every 2 or 3 weeks by intravenous route for cancer treatment [130]. On the other hand, the treatment of ocular diseases implies multiples administrations by intraocular route since half-life of bevacizumab by ocular route is small (between 7-10 days) [131]. Thus, patient compliance to therapy can be compromised [127] due to the possible onset of different complications such retinal detachment, endophthalmitis and vitreous haemorrhage [132].

Antibody-based therapy has several limitations due to large size of antibodies which leads to a limited pharmacokinetics and a low tumor penetration. Also, this type of treatment has the need of multiple administrations, resulting in high doses and an expensive therapy [116]. These drawbacks can be overcome by the encapsulation of bevacizumab into nanocarriers. In recent years, different types of nanosystems have been developed to encapsulate bevacizumab. A recent study showed that encapsulation of bevacizumab in chitosan NPs promotes an inhibitory effect of VEGF [133]. Battaglia *et al.* produced bevacizumab-loaded solid lipid NPs (SLNs) and the results have shown that antiproliferative and antiangiogenic bevacizumab activity in glioblastoma (GBM) treatment was increased 100-200 fold when delivered by SLNs compared to free bevacizumab [134]. Other study successfully encapsulated bevacizumab into nanostructured mesoporous silica films [135]. The use of PLGA NPs as nanosystems to bevacizumab delivery overcome some limitations of antibody-based therapy [114] allowing the modulation of release profile of bevacizumab [130] and potentiate its intracellular delivery to cells [134]. PLGA allows a controlled release of the drug [136] and the antibody release profile by PLGA NPs usually have an initial burst release, attributed to the large molecular size of bevacizumab, followed by a slower release that occurs due to diffusion and degradation of polymer [114, 118]. Previous studies showed that is possible have a sustained release of bevacizumab from PLGA NPs over time [130], once the NPs could be retained in the cytoplasm resulting in sustained intracellular drug levels. In specific, a study showed that bevacizumab was released by polymeric NPs after 30 days of incubation [125] and another study showed a release of bevacizumab over 91 days [116]. It is also known that the release of NPs produced through PLGA 50:50, used in the present work, achieve a complete degradation profile after two months [137]. As well, it was demonstrated that the release profile of bevacizumab is pH-dependent, meaning that the quantity of bevacizumab release increase with higher pHs. Bevacizumab has an isoelectric point of 8.3 and at pH below this value, bevacizumab is positively charged. As PLGA NPs have a negative charge, there is a strong electrostatic attraction between the NPs and the antibody at pH lower than 8.3, decreasing the release rate [130]. A slow release profile of the drug allows a reduction of the frequency of administrations, increasing overall treatment convenience and reducing the cost of therapy.

Chapter II – Aims of the Thesis

The general objective of this dissertation was to design and characterize a NP system to specifically target CRC overexpressing CD44v6. The NPs were produced with low toxicity polymers, PLGA and PEG, to deliver intracellularly bevacizumab to CD44v6 cell-surface receptor overexpressed in cancer cells. This system was functionalized with a human antibody fragment with specificity for CD44v6 overexpressed in mCRC. This targeting system, with a loaded mAb and functionalized with a Fab, has never been made before and intends to be more specific for carcinogenic cells, increasing the efficacy of the drug with lower toxicity in healthy cells.

The specific aims of this dissertation were:

1. Produce and characterize bevacizumab-loaded PLGA-PEG NPs functionalized with v6 Fab;
2. Study the toxicity of NPs in cancer cells with and without overexpression of CD44v6;
3. Characterize biologically the produced NPs for binding specificity and affinity to CD44v6 as a surface receptor of cancer cells;
4. Demonstrate the cell uptake of NPs and evaluate its specificity and affinity to CD44v6;
5. Characterize the intracellular levels of bevacizumab and VEGF after incubation of NPs in CD44v6 expressing cancer cells.

Chapter III – Materials and Methods

1. Materials

The human stomach adenocarcinoma epithelial cell lines MKN74-CD44std and MKN74-CD44v6+ were purchased from Japanese Collection of Research Bioresources (JCRB) Cell Bank, Japan. The Roswell Park Memorial Institute (RPMI) medium and Versene were acquired from ThermoFisher Scientific, USA. The fetal bovine serum (FBS) was purchased from Biochrom AG (Germany) and geneticin was acquired from Santa Cruz Biotechnology (USA). Poly(lactic-*co*-glycolic acid) with 50:50 LA:GA ratio (PLGA 5004 A, 44,000 Da) was kindly offered by Corbion-Purac Biomaterials (Netherlands). Poly(lactic-*co*-glycolic)-b-poly(ethylene glycol)-Maleimide (PLGA-PEG-Mal, 30,000-5,000 Da) and Poly(lactic-co-glycolic acid)-Flamma Fluor FKR648 (PLGA-FKR648, 20,000-30,000 Da) were purchased from PolySciTech (USA). The surfactant Poloxamer 407 (Pluronic® F127) was kindly offered from BASF (USA). The mAb Bevacizumab (Avastin®) was kindly offered by pharmacy of Centro Hospital do Porto. The Amicon centrifuge filters (100 kDa MWCO) were acquired from Merck (USA) and TMB (3,3′,5,5′-Tetramethylbenzidine) substrate from Thermo Fisher Scientific (USA). For the high-pressure liquid chromatography (HPLC) analysis, Trifluoroacetic acid (TFA) from Acros Organics (USA) and Acetonitrile HPLC Gradient Grade from Fisher Scientific (UK) were used. Ethyl acetate (EA) and Triazolyl Blue Tetrazolium Bromide (MTT) were purchased from Sigma (USA). Fab anti-CD44v6 was bought in Bio-Rad (USA). The antibodies used include horse radish peroxidase (HRP)-conjugated goat anti-human secondary antibody (anti-human-HRP), from Milipore (USA), PE (Phycoerythrin) human anti-VEGFA antibody from Abcam (UK) and APC (Allophycocyanin) anti-human IgG Fc were acquired from Biolegend (USA).

2. Methods

2.1. Cell Culture

MKN74 cell line is a human epithelial cell line derived from a moderately differentiated tubular adenocarcinoma (intestinal-type carcinoma) and the gastric cancer cell model system used is based on cells with forced overexpression of CD44v6 in order to ensure gastro-intestinal CD44v6-expressing cell specificity (MKN74-CD44v6+). The cells were modified with an expression vector containing green fluorescent protein (GFP). This

GFP expression of the cells dictated the choice of fluorophore used in cell studies. MKN74 cells with forced CD44v6 expression (MKN74-CD44v6+) were used as testing model and MKN74 cells expressing the standard version of CD44 (MKN74-CD44std) were the control. Previous work validated the utility of modified MKN74 cells, ensuring that the transfected cell model could monitor binding of v6 Fab NPs to the cells [56].

MKN74 cell lines were maintained in RPMI medium supplemented with 10% (v/v) FBS and 0.5 mg/mL geneticin to maintain selection pressure of CD44v6 expressing cells. The cells were sub-cultured when 80% confluency was reached and maintained at 37°C and 5% CO_2 in a water-saturated atmosphere in an incubator.

2.2. Production of PLGA-PEG Nanoparticles

The optimization of the protocol for the encapsulation of bevacizumab in PLGA-PEG NPs was based on work previously developed [130, 137], where PLGA NPs (without PEG) were produced using a modified solvent emulsification-evaporation method based on a w/o/w double emulsion. In double emulsion technique, polymers were dissolved in organic solvent, EA. The hydrophobic solution was then emulsified with an aqueous phase containing the drug to be encapsulated or water, in case of empty NPs. The first created emulsion was added to a surfactant, to form the w/o/w emulsion using sonication. This emulsion was left under magnetic agitation for 3 h at 300 rpm to evaporate the organic solvent. After the 3 h, the NPs formed were separated from the surfactant and non-encapsulated drug by centrifugation.

A work studied the influence of surfactants of ligand-decorated PLGA-PEG NPs on target recognition and showed that PLGA-PEG NPs functionalized with v6 Fab made from 2% Poloxamer 407 had the highest target binding in MKN74-CD44v6+ cells [138]. Thus, all the NPs formulations developed in the present work were produced with 2% Poloxamer 407.

The method was performed with the following percentages: 80% of PLGA 50:50, 10% of PLGA-FKR648 and 10% of PLGA-PEG-Mal. FKR648, a red channel fluorophore with absorbance at 642 nm and emission at 663 nm, was selected to reduce the interference of GFP from the cells with detection of the fluorescent NPs. Twenty mg of total PLGA were dissolved in 1 mL of EA overnight at room temperature (RT). Then, 80 µL of 25 mg/mL bevacizumab solution (Avastin®) were added, and the first emulsion was homogenized for 30 seconds using a Vibra-Cell™ ultrasonic processor with 70% of amplitude. After the primary emulsion, 4 mL of 2% Poloxamer 407 in phosphate buffer at pH 8.3 were added

into the primary emulsion (w/o) and mixed with similar sonication conditions. Finally, the second emulsion (w/o/w) was added into 7.5 mL of the same surfactant solution and left in the fume hood under magnetic stirring at 300 rpm during 3 hours for organic solvent evaporation. Empty PLGA-PEG NPs (without antibody encapsulation) were processed similarly but 80 µL of ultrapure water was used as aqueous phase, instead of antibody solution. Bevacizumab-loaded PLGA-PEG NPs were washed once at 10,000 *x g* for 20 min at 4°C. The obtained empty PLGA-PEG NPs were washed three times with 10 mL ultrapure water using Amicon centrifuge filters (100 kDa MWCO) at 3,000 *x g* during 10 min at 4°C. The final NPs concentrations before functionalization equals to 2 µg/µL. PLGA-FKR648/PEG-Mal NPs that were encapsulated with bevacizumab were termed "bevacizumab-loaded PLGA-PEG NPs" and NPs without drug were called "empty PLGA-PEG NPs". **Figure 6** shows a schematic representation of the NPs production.

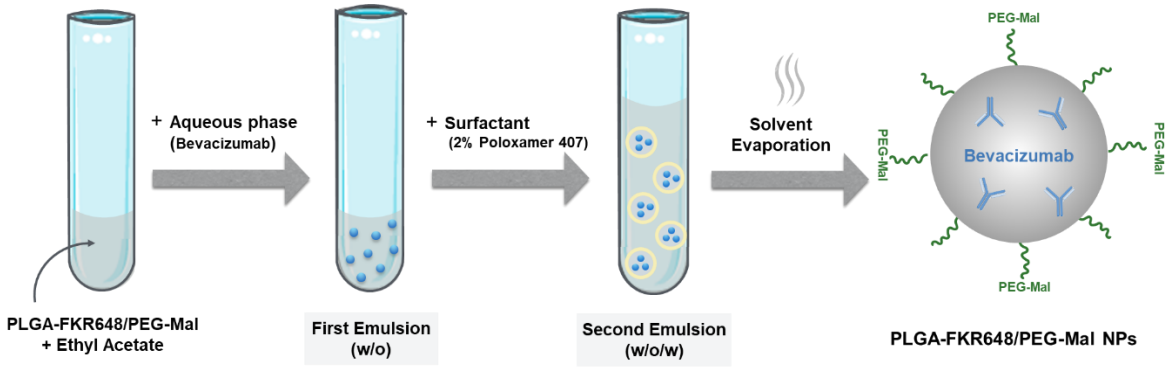

Figure 6. Production of bevacizumab-loaded PLGA-PEG NPs by double emulsion technique. Bevacizumab was added to the polymers dissolved in EA and sonicated to form the first emulsion (w/o). The first emulsion was immediately added to the surfactant solution and sonicated, forming the second emulsion (w/o/w). The evaporation of the organic solvent leads to the formation of NPs.

2.3. Functionalization of Nanoparticles with the Antibody Fragment AbD15179

Previous work tested different molar ratios of Fab:PLGA during Fab conjugation to the PLGA-PEG NPs, to investigate which ratio demonstrate the strongest binding to MKN74-CD44v6+ cells [56]. The results showed that a Fab:PLGA ratio of 1:25 has the better ratio for cell studies and it was the ratio used in this work.

The thiol-Michael addition click based on conjugation to a maleimide functional group was applied to perform the conjugation reaction between the thiol group (-SH) of the three C-terminal cysteines of antibody fragment AbD15179 specific for CD44v6 (v6 Fab), and the maleimide end-groups of PEG chains in the PLGA-PEG NPs (**Figure 7**). Briefly,

Fabs were diluted to reach a final concentration of 1 µM in 1x PBS pH 7.4 and ultrapure water. Then, Fabs were reduced with TCEP (tris(2-carboxyethyl)phosphine) at a final concentration of 3 µM, to allow mild reduction of the C-terminal cysteines and incubated for 1-2 hours at 4°C before NPs addition. To perform the conjugation of the Fab to the maleimide group of NPs, 25 µL of PLGA-PEG NPs at 2 µg/µL were centrifugated at 10,000 *x g* for 10 min at 4°C. The pellet was resuspended in 50 µL of Fab at 1 µM, to maintain a NPs concentration of 1 µg/µL, which equals to a molar ratio of 1:25 Fab:PLGA. NPs without Fab conjugation were processed similarly but with PBS only. After overnight incubation at 4°C, the NPs were washed three times by centrifugation at 10,000 *x g* during 10 min at 4°C with 200 µL of ultrapure water. In the last wash, the NPs were resuspended in 50 µL of ultrapure water. All NPs were maintained in low light conditions, and each formulation was performed in triplicate. PLGA-FKR648/PEG-Mal NPs that were conjugated with the human AbD15179 Fab were termed “v6 Fab-PLGA-PEG NPs”. NPs conjugated with human negative control Fab, called (-) Fab-PLGA-PEG NPs, were produced to ensure that any downstream NP binding were due to CD44v6 specificity and not from the presence of another conjugated protein. NPs without any Fab conjugation were termed “bare PLGA-PEG NPs”.

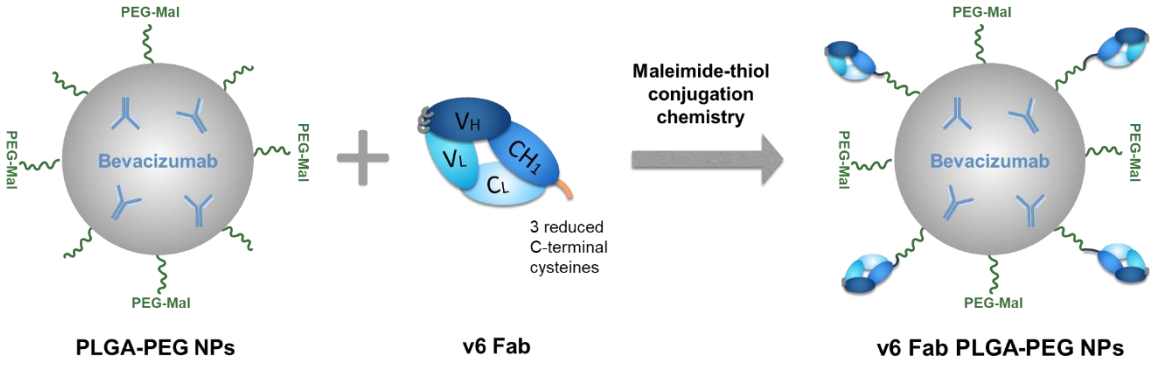

Figure 7. Functionalization of PLGA-PEG NPs surface with v6 Fab through maleimide-thiol conjugation chemistry. v6 Fab was mildly reduced with TCEP and added to the washed PLGA-PEG NPs to produce PLGA-PEG NPs conjugated with a human Fab specific for human CD44v6.

2.4. Physicochemical Characterization of Nanoparticles

NPs were characterized for their hydrodynamic diameter and polydispersity index (PdI) through dynamic light scattering (DLS) method. Zeta potential was measured by electrophoretic light scattering (ELS). Both methods were performed using the Malvern Zetasizer Nano ZS instrument (Malvern Instruments, UK). The samples were diluted 1:100

in sodium chloride (NaCl) 10 mM solution at pH 7.4. Three measurements were taken for each of the triplicate NP formulations.

Transmission electron microscopy (TEM) was used to visualize the morphology of the bare and v6 Fab-PLGA-PEG NPs. All samples were mounted in a copper grill and treated with 2% uranyl acetate (negative staining). The particles were observed through a JEOL JEM-1400 TEM electron microscope (JEOL, USA).

2.5. Determination of Fab Conjugation Efficacy to the Nanoparticles

Enzyme-linked immunosorbent assay (ELISA) was performed to determine the conjugation efficacy of the Fabs to the PLGA-PEG NPs. Briefly, 10 µg of functionalized NPs and non-functionalized NPs (for control purpose) were diluted in 50 µL of 50 mM bicarbonate/carbonate coating buffer at pH 9.6 and added to the 96-well plate in duplicate, for 3 h at 37°C. Blocking was achieved with 100 µL of 1% bovine serum albumin (BSA) in 1x PBS at pH 7.4 for 1 h at 37°C. The Fab was detected with 50 µL of anti-human-HRP diluted 1:5000 in PBS for 1 h at 37°C. 50 µL of TMB substrate was added to the wells, and the reaction was stopped with 50 µL of 2M sulfuric acid. Absorbance at 450 nm was measured with a microplate reader (BioTek Synergy Mx). Between each of the steps, each well was washed three times with 100 µL of PBS containing 0.1% Tween-20 (PBST). A standard curve of known v6 Fab concentrations (200, 100, 50, 40, 25, 15, 10, 6.25, 3.125 and 1.562 ng/µL) was also run in parallel.

2.6. Determination of Bevacizumab Content of Nanoparticles

Association efficiency (AE) and drug loading (DL) are two important parameters to characterize the bevacizumab content of PLGA-PEG NPs. Therefore, the AE and DL were calculated by indirect method. The values of AE and DL were calculated using the following equations 1 and 2, respectively, considering free bevacizumab amount in the supernatant after washing procedure of PLGA-PEG NPs:

$$\mathrm{AE}\ (\%) = \frac{\text{total amount of bevacizumab} - \text{free bevacizumab in supernatant}}{\text{total amount of bevacizumab}} \times 100 \qquad (1)$$

$$\mathrm{DL}\ (\%) = \frac{\text{total amount of bevacizumab} - \text{free bevacizumab in supernatant}}{\text{total dry weight of nanoparticles}} \times 100 \qquad (2)$$

A validated reversed-phase high pressure liquid chromatography (RP-HPLC) method with fluorescence detection [139] was used to evaluated indirectly the bevacizumab

payload from fresh PLGA-PEG NPs. Measurements were perform using a Shimadzu UFLC Prominence System coupled with a Shimadzu RF-10AXL fluorescence detector with excitation wavelength at 280 nm and emission at 360 nm. For HPLC analysis, it was used a Zorbax SB 300SB-C8 Narrow-bore column with 5 µm particle size, 2.1 mm internal diameter x 260 mm length from Agilent Technologies (Santa Clara, CA, USA). The mobile phase consisted of 0.1% TFA in ultrapure water (eluent A) and 0.1% TFA in acetonitrile (eluent B) at a flow rate of 1.0 mL/min in a gradient mode. The gradient started at 35% of eluent B for 1 min, was increased to 45% in 0.1 min and kept constant from 1.1 to 6 min. Eluent B was then decreased to 35% in 0.1 min and kept constant from 6.1 to 14 min. The temperature of the column was maintained at 75 °C and the injection volume was 2 µL. The total area of the peak was used to quantify bevacizumab. A standard curve of known bevacizumab concentrations (1, 5, 10, 25, 50, 75 and 100 µg/mL) was also run in parallel.

2.7. Nanoparticles Cytotoxicity

To test the cytotoxicity of the NPs, MTT assay was performed in MKN74-CD44std and MKN74-CD44v6+ cell lines. To assess the ideal cell density for the MTT assay, it was performed a calibration curve for both cell lines. MKN74-CD44std and MKN74-CD44v6+ cells were seeded at 8,000 and 6,000 cells/well, respectively, in 96-well plates and incubated for 24 h in a cell incubator at 37°C and 5% CO_2. The culture medium was removed, replaced with 200 µL of different concentrations of NPs (5 and 50 µg/mL) or free bevacizumab (0.5 and 5 µg/mL) dissolved in supplemented RPMI medium in each well and incubated for 24 h at 37°C in a 5% CO_2 air atmosphere. For control purpose, cultured cells were treated with supplemented medium (positive control), 1% (v/v) Triton-X in supplemented medium (negative control), and for the background, wells of each plate were devoted with supplemented medium only, without cells. After 24 h, the cells were washed three times with PBS, replaced with 200 µL of MTT solution per well (at a final concentration of 0.5 mg/mL in supplemented RPMI medium) and incubated for 4 h at 37°C in a 5% CO_2 air atmosphere. The reaction was stopped by removing the medium and adding 200 µL of dimethyl sulfoxide (DMSO). After 20 minutes of shaking at RT in the dark, the plate was measured with a microtiter plate reader (BioTek Synergy Mx) at 570 nm and 630 nm absorbance. The values of 630 nm absorbance were subtracted from the values of 570 nm absorbance, and this subtracted value was used to calculate the percentage of cell viability following the equation 3.

$$\text{Cell viability } (\%) = \frac{\text{experimental value} - \text{negative control}}{\text{positive control} - \text{negative control}} \times 100 \qquad (3)$$

2.8. Binding of Nanoparticles to the Surface of Cells Expressing CD44v6

Fluorescence-activated cell sorting (FACS) was performed to determine binding of the NPs to the surface of MKN74 cells with or without overexpression of CD44v6. Cells seeded in a T-75 flask with ~80% confluency were detached with versene and fixed with 0.1% sodium azide (NaN_3) in PBS supplemented with 10% FBS for 30 min. Hundred thousand cells per well were added to a 96-well plate with round-bottom wells and 50 µg/mL of bare, (-) Fab and v6 Fab-PLGA-PEG NPs were incubated with the cells for 2 h, followed by three washes with PBS. All the steps took place on ice. The binding of NPs to the surface of cells was determined by measuring the intensity of the red channel fluorophore FKR648 with the BD Accuri™ C6 Plus (BD Biosciences). The data was analysed with FlowJo v10 by determination of mean fluorescence intensity (MFI).

2.9. *In Vitro* Cell Uptake Studies

To perform *in vitro* internalization studies, MKN74-CD44v6+ and MKN74-CD44std were seeded at 40,000 cells/well in 24-well plates in RPMI complete medium and cultured for 24 h at 37°C and 5% CO_2. After 24 h, 50 µg/mL of NPs (bare NPs, (-) Fab-PLGA-PEG NPs and v6 Fab-PLGA-PEG NPs) were added to each well in RPMI medium without the FBS and geneticin supplements. As control, the cells were maintained in medium (cells only). After incubation, the cultured cells were washed twice with PBS, detached with Trypsin/EDTA (T/E) and centrifugated at 1300 rpm for 7 min at 4°C. After the discard of supernatant, the cells were washed in PBS and centrifugated once more to resuspended in 100 µL of PBS in order to analyse immediately by flow cytometry. Fluorescence intensity of the red channel fluorophore FKR648 was measured with the BD Accuri™ C6 Plus (BD Biosciences). The data was analysed with FlowJo v10 by determination of MFI.

2.10. Intracellular Staining of Bevacizumab and VEGF

To assess if bevacizumab-loaded PLGA-PEG NPs were internalized in cells and to evaluate the intracellular levels of VEGF upon bevacizumab treatment, it was performed a protocol to study the intracellular levels of bevacizumab and VEGF after the incubation of NPs in MKN74-CD44v6+ cells. Three hundred thousand of cells/well were seeded in 1 mL of RPMI medium supplemented in 6-well plates and cultured for 24 h at 37°C and 5% CO_2. In the next day, the cells were either maintained in medium without supplements (cells only) or incubated with 50 µg of (-) Fab or v6 Fab bevacizumab-loaded PLGA-PEG NPs, in RPMI

without supplements, for 24 h at 37°C and 5% CO_2 atmosphere. As another control, cells were also incubated with the same quantity of free bevacizumab that was present at the concentration of incubated NPs.

After 20 h of cell seeding, a cell stimulation cocktail was added to the cells in RPMI medium without supplements. The cell stimulation cocktail consisted in a mixture of 50 ng/mL of PMA (phorbol 12-myristate 13-acetate), 500 ng/mL of ionomycin and 10 µg/mL of Brefeldin A. PMA and ionomycin activated the cells leading to cytokines production that are captured in the rough endoplasmic reticulum and Golgi apparatus. This localization of cytokines is caused by the protein transport inhibitor Brefeldin A, which blocks intracellular protein transport, thus allowing intracellular detection of the secreted proteins by immunofluorescent staining [140]. After 24 h of the NPs incubation, the medium was collected to a tube and the cells were detached with ice cold PBS with the help of a scrapper. Then, the cells were removed to the same falcon and centrifuged at 1200 rpm for 5 min at 4°C. The supernatant was discarded, the cells were resuspended in PBS and the same volume of 4% paraformaldehyde (PFA) was added. The incubation took place at RT, in the dark, for 20 minutes. After the fixation step, the cell suspension was centrifuged once more and resuspended in 1 mL of FACS buffer (PBS/sodium azide/BSA).

Two hundred thousand cells/well (~200 µL) were plated in 96-well plate with round-bottom wells and centrifuged at 2000 rpm for 10 seconds at 4°C. The supernatant was discarded, and the cells were incubated with 200 µL of permeabilization buffer (10% saponin/FACS buffer) for 10 minutes at ice. Then the cells were centrifuged at 2000 rpm for 10 seconds at 4°C. After discard the supernatant, it was added in each well 30 µL of intracellular antibody (Recombinant Anti-VEGFA antibody and APC anti-human IgG Fc antibody) diluted at 1:30 in permeabilization buffer and incubated 20 minutes at ice, in the dark.

To stain intracellular VEGF levels, it was used a PE human anti-VEGFA antibody, diluted at 1:30, which was detected by flow cytometry by the fluorescent protein label PE. For bevacizumab staining, APC anti-human IgG Fc antibody at a dilution of 1:30 was used. This antibody was detected by flow cytometry by the fluorescent protein label APC. The tested samples (cells only, free bevacizumab, (-) Fab and v6 Fab bevacizumab-loaded PLGA-PEG NPs) were incubated with a mixture of the antibodies.

To stop the incubation, 200 µL of FACS buffer was added, the cells were centrifuged one more time at 2000 rpm for 10 seconds at 4°C and resuspended in 100 µL of FACS buffer. Therefore, the cells were posteriorly stored at 4°C, protected from light, and

analysed as soon as possible with the BD Accuri™ C6 Plus (BD Biosciences). The data was analysed with FlowJo v10.

2.11. Statistical Analysis

Statistical analysis was performed by the GraphPad Prism Software version 8.0.2. Normally was evaluated using Shapiro-Wilk test. Differences between groups were analysed by one-way ANOVA with Dunnett's multiple comparisons test. The statistical differences were considered significative at * $p< 0.05$; very significative at ** $p < 0.01$; highly significative at *** $p < 0.001$ and extremely significative at **** $p < 0.0001$.

Chapter IV – Results and Discussion

The objective of this work was to produce and characterize PLGA-PEG NPs loaded with bevacizumab and conjugated with a human Fab specific for CD44v6 expressing CRC cells, for an intracellular delivery of the drug with lower toxicity. Initially, NPs were produced and characterized regarding size, charge and shape and its toxicity was evaluated in cancer cells. Then, the specificity of v6 Fab-PLGA-PEG NPs was tested in cancer cells overexpressing CD44v6, namely the binding to the cell surface and the cell uptake. Lastly, it was evaluated the ability of NPs deliver bevacizumab intracellularly and its anti-angiogenic activity through VEGF levels.

1. Physicochemical Characterization of Nanoparticles

Modified solvent emulsification-evaporation method based on a w/o/w double emulsion technique was the method used to produce empty and bevacizumab-loaded PLGA-PEG NPs. All NPs formulations were characterized after production regarding particle size, PdI and surface charge (**Table 1** and **Figure 8**). Mean particle size (Z-average or hydrodynamic radius) and surface charge (Zeta potential) are the two most commonly mentioned factors that are responsible for a range of biological effects of NPs [141] and were measured by DLS and ELS, respectively. Zeta potential is the potential at the slipping/shear plane of a colloid particle moving under electric field, and its widely used to assess the surface charge of NPs. PdI was used to characterize the NP size distribution, where small values of PdI (near to zero) confirm the uniformity of size distribution.

Table 1. Physicochemical characterization of the PLGA-PEG NPs. Z-average (size), polydispersity index (PdI) and Zeta-potential (charge) of the empty and bevacizumab-loaded PLGA-PEG NPs, with or without functionalization with v6 Fab, measured by DLS and ELS. Values represent mean ± standard deviation (n=3).

Formulation	Bevacizumab	Z-average (size, nm)	Polydispersity Index (PdI)	Zeta Potential (charge, mV)
Bare PLGA-PEG NPs	-	124.1 ± 0.1	0.098 ± 0.015	-4.5 ± 0.2
	+	183.5 ± 4.9	0.388 ± 0.044	-6.4 ± 1.1
(-) Fab-PLGA-PEG NPs	-	167.2 ± 2.5	0.235 ± 0.005	-6.1 ± 0.8
	+	253.5 ± 1.4	0.353 ± 0.003	-9.8 ± 0.1
v6 Fab-PLGA-PEG NPs	-	245.4 ± 2.9	0.186 ± 0.013	-8.2 ± 0.5
	+	345.8 ± 16.4	0.382 ± 0.072	-12.0 ± 0.9

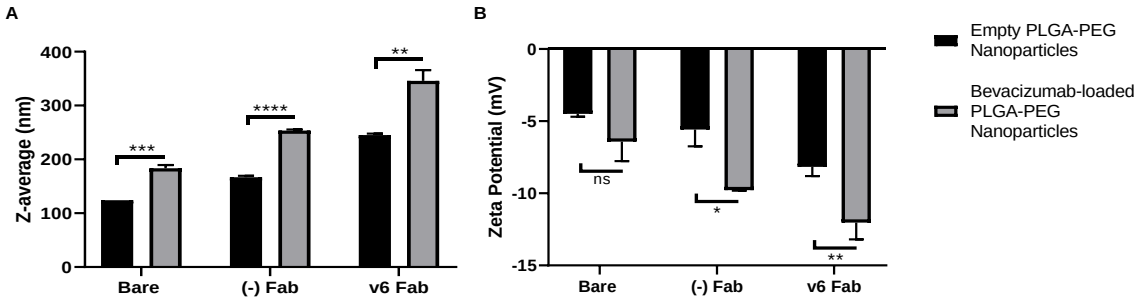

Figure 8. Comparison of (A) size and (B) charge between empty and bevacizumab-loaded PLGA-PEG NPs. In both graphs, bars represent mean values ± standard deviation (n=3). The statistical differences are given for non-significant (ns) at $p > 0.05$; significative at * $p < 0.05$; very significative at ** $p < 0.01$; highly significative at *** $p < 0.001$ and extremely significative at **** $p < 0.0001$.

Before proceeding with encapsulation of bevacizumab into PLGA-PEG NPs and functionalization of bevacizumab-loaded PLGA-PEG-NPs, the empty PLGA-PEG NPs were produced and functionalized with v6 Fab. The empty v6 Fab-PLGA-PEG NPs show an increase in size and decrease in charge than the ones without any Fab. This possibly indicates the presence of the v6 Fab at the surface of the NPs. To confirm the functionalization of NPs with the v6 Fab, it was performed an ELISA. The values were interpolated from a standard curve with known v6 Fab concentrations (**Figure S1**) and the

results showed a conjugation efficiency of 86.08 ± 5.53%. This result demonstrated that the conjugation of the v6 Fab to the surface of PLGA-PEG NPs was effective.

The initial protocol to produce bevacizumab-loaded PLGA-PEG NPs consisted in the use of 80% of PLGA-COOH, 10% of PLGA-PEG-Mal, 10% of PLGA-FKR648 and as surfactant, 2% (w/v) of Poloxamer 407 dissolved in ultrapure water at pH 7.4. However, the NPs produced with these conditions showed a size near 400-500 nm and a PdI near 0.5 before the washing steps. After the washes, the size and PdI increased even more, making functionalization with the antibody fragment impossible. Several hypotheses were placed that could be carrying such a large particle size, namely the amount of antibody introduced into the particle in relation to the PLGA mass, and the existence of reactivity between the PEG-Mal chemical group and the bevacizumab. Therefore, to discard those hypotheses, different types of PLGA (PLGA-PEG-NH_2 and PLGA-PEG-COOH) and different concentrations of the aqueous phase were tested. However, the particle size remained at 400-500 nm prior to washes (data not shown). Next, it was tested the production of PLGA-PEG NPs with 2% Poloxamer 407 prepared in phosphate buffer instead of ultrapure water, at pH 8.3, which is the isoelectric point of bevacizumab. This pH was chosen to verify if the stability of formulations was affected and to increase the theoretical AE. The surfactant solution made in buffered solution, instead of made in water, allows the maintenance of the pH imposed during the NPs production and purification.

The bevacizumab-loaded PLGA-PEG NPs produced with 2% Poloxamer 407 at pH 8.3 showed a decrease on NPs size for approximately 180-190 nm (**Table 1**), which suggests that the stability of formulations was affected. At the isoelectric point of bevacizumab (pH 8.3), the sum of all its electrical charges is zero and above this value bevacizumab is negatively charged. Therefore, as molecules are practically neutral at pH 8.0, the solubility of bevacizumab decreases leading to the onset of monodisperse particles and to an increase in AE of the antibody. However, in comparison with the empty PLGA-PEG NPs, the encapsulation of bevacizumab increases the mean particle size and the PdI (**Table 1**), meaning that the particle size distribution is heterogeneous. The functionalization of bevacizumab-loaded PLGA-PEG NPs increases even more the size of the systems. These results may be due to the high size of bevacizumab (149 kDa) and absorption of the antibody on the NPs surface. The encapsulation of proteins through w/o/w method in PLGA-PEG NPs can lead to the loss of therapeutic efficacy of the protein due to its degradation/denaturation [90, 118]. The protein stability can be affected once the protein is exposed in water-organic interface and the homogenization is also a critical step in the process.

All the formulations presented an overall surface charge negative close to neutral. Some negative values may be attributed to the acidic properties of PLGA [69]. Zeta potential values near to zero are attributed to PEG, which have neutral charge, and when measurements are made with sodium chloride solution, the zero values are more evident comparatively with measurements made with ultrapure water [142].

In summary, the produced NPs have a mean size in the range of 200-300 nm, a PdI between 0.1 and 0.4 and a zeta potential between -5 and -10 mV. All types of NPs formulations demonstrated mean particle sizes that are considered to be suitable for intravenous administration. It has been shown that very small particles can be cleared rapidly from the systemic circulation by renal filtration [143] while bigger NPs have the potential to become entrapped inside organs of RES, such as liver, spleen and bone marrow [144]. After intravenous administration of positively charged NPs, the presence of serum proteins can lead to the aggregation of NPs, creating protein corona [145]. These aggregates can often be entrapped inside RES organs or cause embolism in blood capillaries [146]. For that reason, a negative surface zeta potential values of NPs are preferential for long-circulating NPs in the blood [143].

Transmission Electron Microscopy (TEM) was used to evaluate the morphology of NPs formulations (**Figure 9**). NPs showed a spherical appearance and a big range of NPs size.

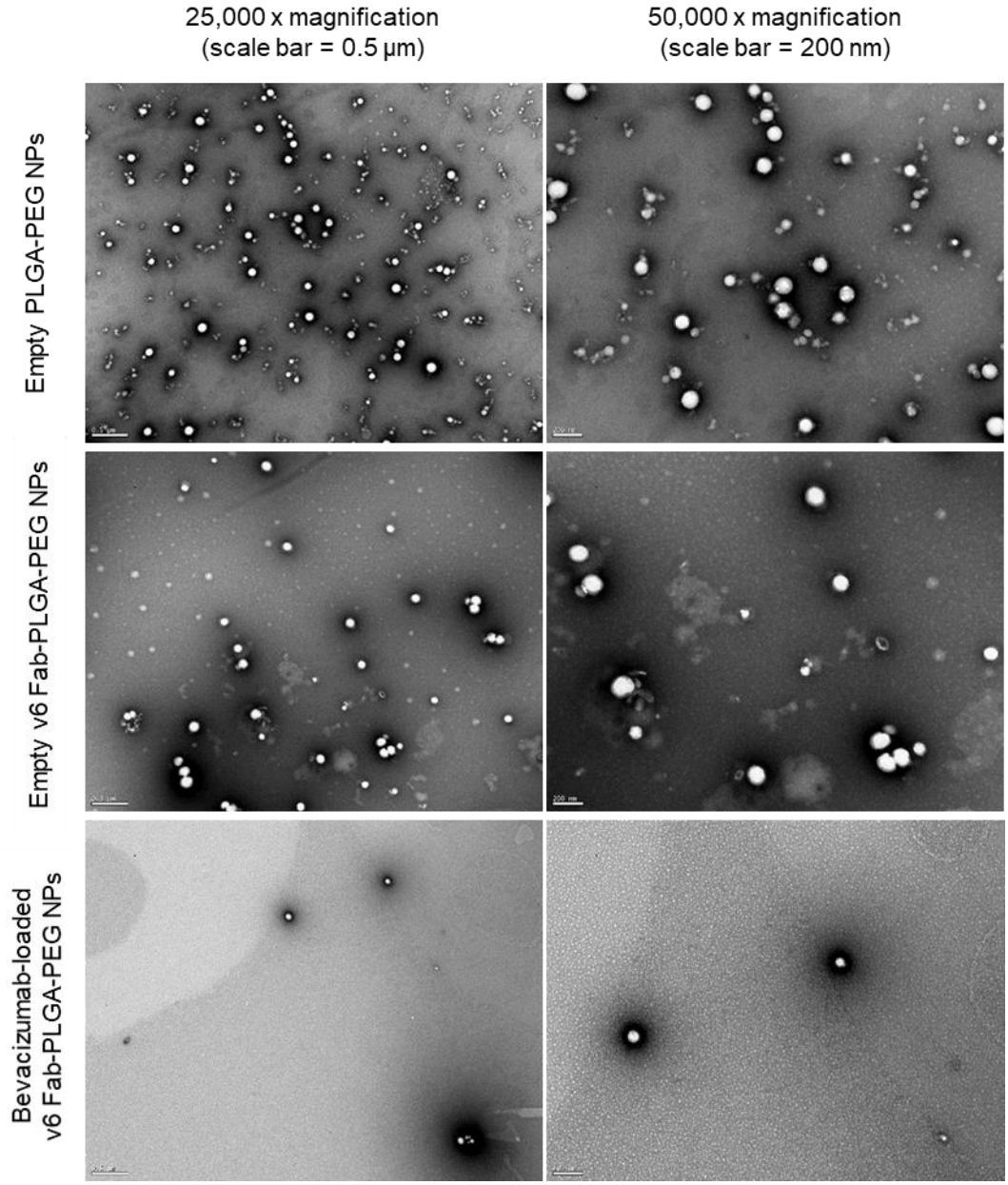

Figure 9. TEM images of the bare and v6 Fab-PLGA-PEG NPs.

2. Bevacizumab Content of Nanoparticles

The AE and DL of bevacizumab for PLGA-PEG NPs were evaluated indirectly by a validated RP-HPLC method with fluorescence detection [139] and the values were interpolated from a standard curve (**Figure S2**) with known concentrations of bevacizumab. The values of bevacizumab-loaded PLGA-PEG NPs showed an AE of 86.52 ± 1.77% and a DL of 7.87 ± 0.16%. Indeed, this production protocol of bevacizumab-loaded PLGA-PEG NPs demonstrated to effectively encapsulate bevacizumab.

In order to check if any antibody was lost in the functionalization process, the bevacizumab content of v6 Fab bevacizumab-loaded PLGA-PEG NPs was also evaluated. However, it was not possible to verify the peak area because the values were residual. A comparison of the peaks of the functionalized particles was made with a water sample (**Figure S3**). This may have happened since a very small volume of the formulation at 2 µg/µL (25 µL) was used to proceed to functionalization process.

3. Nanoparticles Cytotoxicity

In order to assess the cell toxicity of the NPs formulations, the percentage of cell viability was measured using the MTT reduction assay. First, the cytotoxicity of the empty PLGA-PEG NPs was evaluated (**Figure 10**). Then, it was evaluated the toxicity of bevacizumab-loaded PLGA-PEG NPs and free bevacizumab, for comparison purposes (**Figure 11**). The cell lines MKN74-CD44std and MKN74-CD44v6 were used to test cytotoxicity after 24 h of NPs incubation.

It is expected that cell viability would decrease with higher concentrations of bevacizumab and NPs, as can be seen in all conditions, in both cell lines. However, it was observed more cytotoxicity for bevacizumab-loaded PLGA-PEG NPs which is also expected since treatments with bevacizumab are associated with toxicity. Even though, these NPs are less toxic than free bevacizumab at the same concentrations (PLGA-PEG NPs concentration of 5 and 50 µg/mL correspond to, approximately, 0.5 and 5 µg/mL of bevacizumab, respectively).

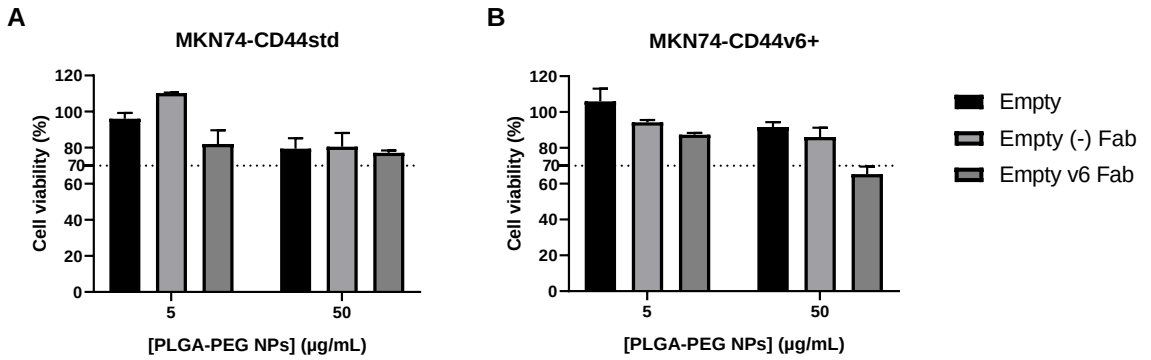

Figure 10. Cytotoxicity of empty PLGA-PEG NPs in (A) MKN74-CD44std and (B) MKN74-CD44v6+ cell lines. NPs concentration of 5 and 50 µg/mL correspond to, approximately, 0.5 and 5 µg/mL of bevacizumab, respectively. The values are represented as mean and error bars represent the standard deviation. n=3 replicates. The dashed line presents 70% of the control value and values below are considered cytotoxic.

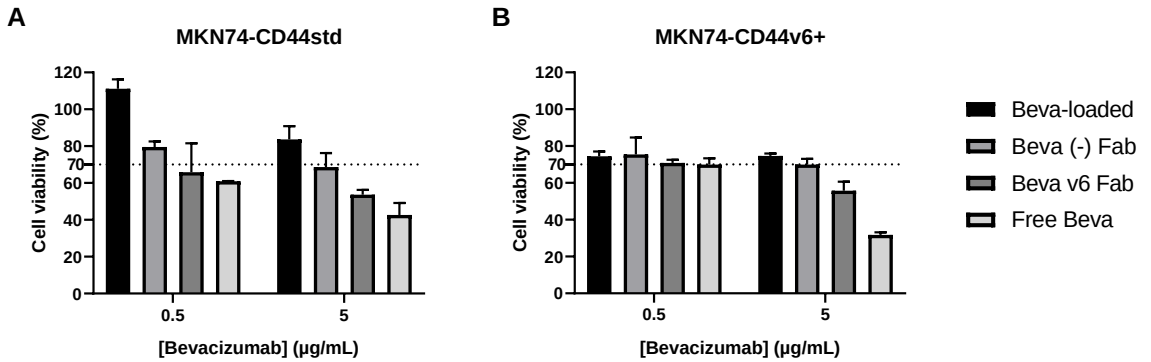

Figure 11. Effect of bevacizumab-loaded PLGA-PEG NPs and free bevacizumab in (A) MKN74-CD44std and (B) MKN74-CD44v6+ cells. The values are represented as mean and error bars represent the standard deviation. n=3 replicates. The dashed line presents 70% of the control value and values below are considered cytotoxic.

It is standardized that if cell viability is reduced to < 70%, the compounds have a cytotoxic potential. In this way, this NP system is not cytotoxic and the NPs with bevacizumab encapsulated are less toxic to the cells in comparison with the free drug. These results are in agreement with literature, that show that PLGA NPs do not present toxicity in both endothelial [130] and epithelial cell lines [147].

4. Specific Binding of v6 Fab-PLGA-PEG Nanoparticles to the Surface of Cells

In this work, the NPs functionalization was performed to trigger the specific recognition of CD44v6 expressed on the surface of cancer cells. To confirm the specific

binding of v6 Fab-PLGA-PEG NPs to CD44v6 in cells, it was performed a protocol to evaluate the binding of the NPs to the cell surface overexpressing CD44v6 by FACS. MKN74-CD44v6+ cells were first detached with versene to impair receptor degradation and the use of sodium azide on the fixation process minimizes surface receptor recycling, meaning that the receptor on the cell surface was maintained to study the real binding of the NPs to the surface receptor.

Figure 12 show the results of empty PLGA-PEG NPs (Figure 12A) and bevacizumab-loaded PLGA-PEG NPs (Figure 12B). First, empty PLGA-PEG NPs functionalized with v6 Fab were tested and then proceeded to bevacizumab-loaded PLGA-PEG NPs functionalized with v6 Fab. For both conditions, the proper negative controls were implemented. The assay was performed with the negative control Fab ((-) Fab-PLGA-PEG NPs) and a non-expressing cell line to ensure that any NP binding increase in MKN74-CD44v6+ cell line was due to CD44v6 specificity.

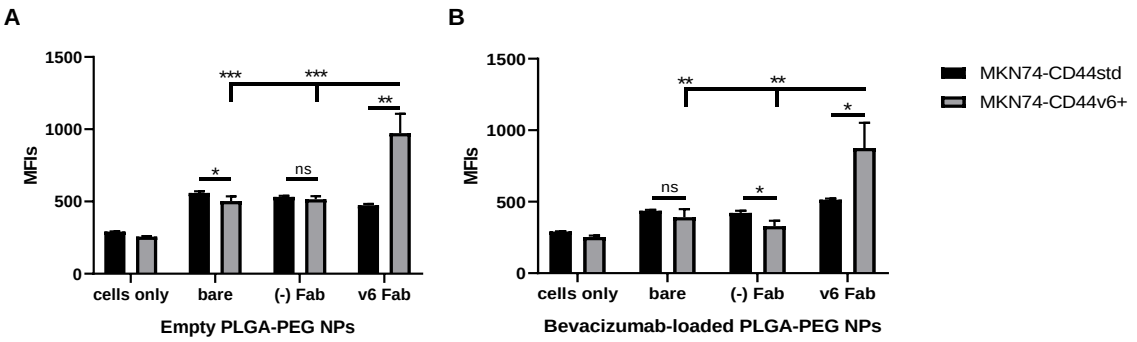

Figure 12. Binding of (A) empty PLGA-PEG NPs and (B) bevacizumab-loaded PLGA-PEG NPs to CD44v6 on the surface of MKN74-CD44std and MKN74-CD44v6+ cells. The values are represented as mean and error bars represent the standard deviation. n=3 replicates. MFIs = mean fluorescence intensity. The statistical differences are given by ** $p < 0.01$; *** $p < 0.001$.

MKN74-CD44std cells showed an increased binding to the surface for the bare and (-) Fab empty PLGA-PEG NPs in comparation with empty v6 Fab-PLGA-PEG NPs. This demonstrates that empty v6 Fab-PLGA-PEG NPs do not have specificity for cells that express CD44std. However, for the bevacizumab-loaded v6 Fab-PLGA-PEG NPs it is possible observe a positive significant difference of the binding to the surface of MKN74-CD44std cells. Though, the difference for these NPs in MKN74-CD44v6+ cells is more evident. There was a significant increase in surface binding for v6 functionalized NPs of empty and bevacizumab-loaded PLGA-PEG NPs compared to bare and (-) Fab NPs in MKN74-CD44v6+ cells, and to v6 functionalized NPs in MKN74-CD44std cells. These

differences confirmed the presence of v6 Fab on the NPs. Nevertheless, bare and (-) Fab NPs show some cell binding to the CD44v6 cells. This can be explained by the fact that MKN74-CD44v6+ cells are modified with a CD44v3-10 variant, that is, there is an overexpression of v6 but also some expression of the other variants between 3 and 10. That way, is expected a residual binding of the nonspecific NPs to cell receptors.

In summary, it is possible to see that v6 Fab-PLGA-PEG NPs have a two-fold increase in cell binding compared to non-functionalized NPs, confirming the specificity of v6 functionalized NPs to CD44v6 surface receptor. Furthermore, Figure 11B shows that the specificity of v6 Fab-PLGA-PEG NPs is maintained with the encapsulation of bevacizumab.

5. Cell Uptake Studies

To ensure that the NPs maintained the specific binding to CD44v6 in live cells, cell uptake studies were performed in the same cell lines with the same concentrations of NPs. The results were analysed by FACS.

Figure 13 shows that v6 Fab-PLGA-PEG NPs, both empty (Figure 13A) and bevacizumab-loaded (Figure 13B), appear to exhibit a higher significant internalization in MKN74-CD44v6+ cells compared with bare and (-) Fab PLGA-PEG NPs, which suggest the ability of the v6 functionalized NPs to be internalized more easily than the non-functionalized NPs. Additionally, v6 functionalized NPs showed a significantly higher uptake in MKN74-CD44v6+ cells than MKN74-CD44std cell line, reinforcing the specificity of v6 Fab NPs to CD44v6 receptor.

Bare and (-) Fab of empty PLGA-PEG NPs are more internalized than the same conditions of bevacizumab-loaded PLGA-PEG NPs. The particle size of empty bare and (-) Fab PLGA-PEG NPs is around 120-170 nm, while bare and (-) Fab bevacizumab-loaded PLGA-PEG NPs have a particle size of 180-250 nm. These particle size differences may influence the rate of NPs internalization in cells, since the small size of empty PLGA-PEG NPs can provide a faster cell uptake compared to bevacizumab-loaded PLGA-PEG NPs.

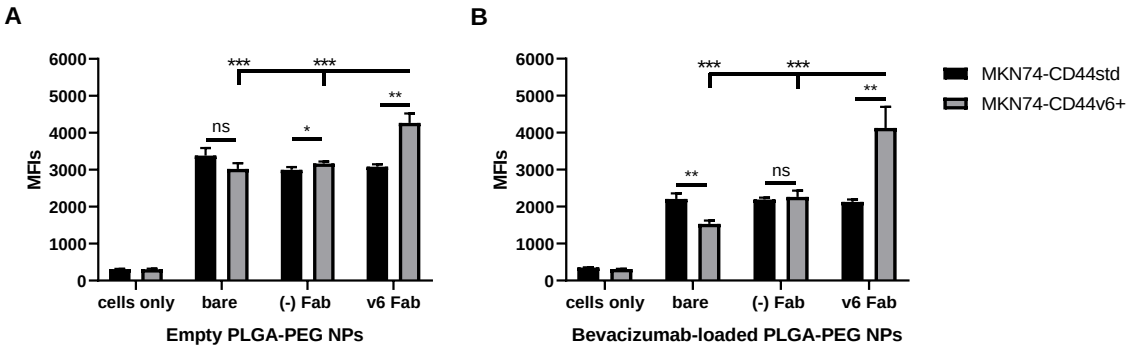

Figure 13. Binding of (A) empty PLGA-PEG NPs and (B) bevacizumab-loaded PLGA-PEG NPs to live cells. The values are represented as mean and error bars represent the standard deviation. n=3 replicates. MFIs = mean fluorescence intensity. The statistical differences are given by *** $p < 0.001$.

The results presented in **Figure 13** are in agreement with the previous experience of the binding to the surface (**Figure 12**). In this work, the NPs were produced to target actively CD44v6 receptor. NPs seems to reach the right target via specific interaction between the targeting v6 Fab on the surface of NPs and CD44v6 receptor on the cell membrane. This specific recognition promotes the particle internalization.

6. Evaluation of Intracellular Levels of Bevacizumab and VEGF

Bevacizumab is a mAb that binds to intracellular VEGF-A and inhibits its interaction with VEGF receptor tyrosine kinases [44], inhibiting the angiogenesis process. Bevacizumab-loaded PLGA-PEG NPs functionalized with v6 Fab aim to intracellularly deliver bevacizumab in order to interact with intracellular VEGF. As previously mentioned, v6 Fab-PLGA-PEG NPs were internalized by CD44v6 expressing cancer cells, so the next step was to study bevacizumab internalization and its bioactivity through interaction with intracellular VEGF.

To evaluate the intracellular levels of bevacizumab and VEGF, MKN74-CD44v6+ cells were incubated with bevacizumab-loaded v6 Fab-PLGA-PEG NPs, and free bevacizumab and bevacizumab-loaded (-) Fab-PLGA-PEG NPs, to serve as controls. After 24 h of incubation, the cells were stained for intracellular VEGF levels with PE human anti-VEGFA antibody and for intracellular bevacizumab with APC anti-human IgG Fc antibody and analysed by FACS.

From **Figure 14**, it can be seen that intracellular levels of bevacizumab in the cells were significant lower after free bevacizumab incubation compared to the bevacizumab-

loaded v6 Fab-PLGA-PEG NPs. On the other hand, intracellular levels of bevacizumab were also significantly higher in the cells incubated with v6 Fab-PLGA-PEG NPs compared to (-) Fab-PLGA-PEG NPs. This means that the v6 Fab-PLGA-PEG NPs were able to internalize and deliver the drug to cells, validating the specificity of v6 Fab to CD44v6 expressing cells.

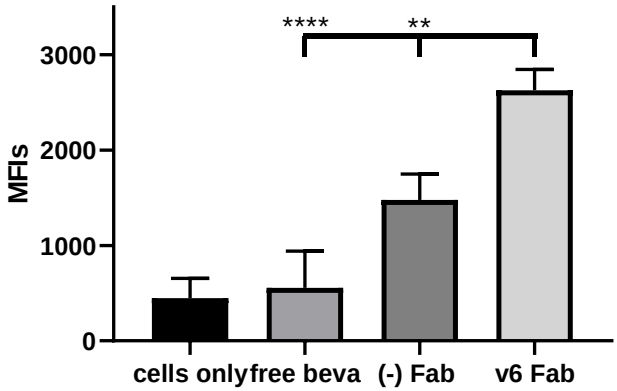

Figure 14. Intracellular fluorescence levels of bevacizumab in MKN74-CD44v6+ cell line, after incubation with free bevacizumab, (-) Fab and v6 Fab bevacizumab-loaded PLGA-PEG NPs. The values are represented as mean and error bars represent the standard deviation. n=3 replicates. MFIs = mean fluorescence intensity. The statistical differences are given by ** $p < 0.01$; **** $p < 0.0001$.

Additionally, other works regarding intracellular delivery of drugs with conjugated NPs have been developed. PLGA-PEG NPs conjugated with folate and loaded with a chemotherapeutic drug, PTX, were showed to be significantly more effective compared to non-targeted NPs in an ovarian peritoneal metastasis model overexpressing folate receptor [148], a growth factor receptor involved in invasion and proliferation of tumors [149]. Farokhzad *et al.* developed NPs produced with PLGA-PEG that were encapsulated with docetaxel (DTX) and functionalized with a RNA aptamer specific for the prostate-specific membrane antigen (PMSA), an antigen expressed on the surface of prostate cancer cells. This targeting system demonstrated to have higher efficacy and reduced toxicity of the drug when compared with non-targeted NPs [150]. A study developed immunoliposomes conjugated with anti-HER2 mAb fragment and loaded with dox, to selective target breast cancers with overexpression of HER2 (human epidermal growth factor receptor 2), a cell surface receptor that plays an important role in progression of breast cancers, among others [151]. The results showed that anti-HER2 immunoliposomes internalized efficiently in cells overexpressing HER2, both increasing drug efficacy and reducing systemic toxicity.

The results presented so far in this dissertation are in line with previously developed work, since PLGA-PEG NPs functionalized with v6 Fab showed to do an effective intracellular delivery of bevacizumab to CD44v6 overexpressing cancer cells.

Then, percentage of intracellular VEGF expressed in cells was studied and the **Figure 15** showed no significance between the groups. However, although not significant, it is possible to observe a tendency in the decrease of intracellular VEGF levels due to the bevacizumab internalization. A possible explanation for this, is the fact that IgG derived fragments, such Fabs, present a higher ability of tissue penetration than full IgG [127]. More significant differences may not have been seen since the concentration of bevacizumab incorporated in cells was very low.

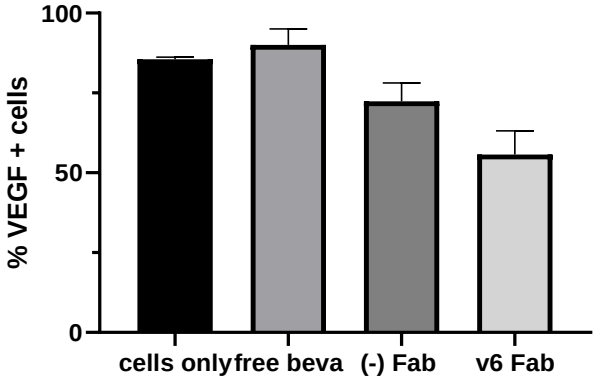

Figure 15. Percentage of VEGF in MKN74-CD44v6+ cells, after incubation with free bevacizumab, (-) Fab and v6 Fab bevacizumab-loaded PLGA-PEG NPs. The values are represented as mean and error bars represent the standard deviation. n=3 replicates.

Anti-angiogenic effects of bevacizumab-loaded PLGA NPs in GBM treatment were studied by Sousa *et al.* after intranasal administration of NPs in an orthotopic GBM nude mice model [152]. The study showed a significant decrease of VEGF levels with bevacizumab-loaded PLGA NPs compared to the free bevacizumab after 2 weeks of treatment. In the present work, the experiment was done only with a 24 h time point and it was already been shown that bevacizumab release profile is slow [116, 125]. Therefore, the biological effect of bevacizumab in decreasing the cellular levels of VEGF may be time dependent, which may explain the non-significant difference in VEGF levels after incubation with free bevacizumab and bevacizumab-loaded PLGA-PEG NPs. As further work, more time points following the treatment of MKN74-CD44v6+ cells with bevacizumab-loaded PLGA-PEG NPs could be added to the experiment in order to evaluate more extensively the anti-angiogenic effect of bevacizumab.

In summary, this study demonstrated that intracellular delivery of bevacizumab was efficiently achieved with v6 functionalized PLGA-PEG NPs and that efficacy of the cell uptake was higher with v6 functionalized NPs targeted to CD44v6 expressing cancer cells.

Chapter V – Conclusions and Future Perspectives

1. Conclusions

CRC is one of the deadliest cancers worldwide due to its metastatic potential. CD44v6 is a transmembrane protein that plays an important role in the establishment of tumors and metastasis, which made this molecule a potential target for therapy and/or diagnosis of tumors. Standard chemotherapy regimens recommend for metastatic stages of CRC are often associated with severe side effects once they do not target a molecule specifically, acting also against the healthy tissues and cells. Targeted therapies combined with nanomedicine have been emerged as a strategy in detecting and target specific molecules that are overexpressed in cancer, such CD44v6. Targeting ligands based on recombinant mAbs are the most commonly used due to their affinity, specificity and engineering malleability.

The therapeutic proposed here is a novel intravenous targeted therapy for mCRC with overexpression of CD44v6. The main objective of this work was to develop and characterize technologically and biologically PLGA-PEG NPs loaded with a mAb and functionalized with a human antibody fragment with specificity for CD44v6.

The rationale of v6 Fab-PLGA-PEG NPs displays qualities as a potential nanocarrier to target CD44v6. PLGA is one of the most polymers used for NPs formulations because is considered biodegradable, biocompatible, allow sustained drug release, have low toxicity and is approved by FDA/EMA. Incorporation of PEG turns the formulation less immunogenic and minimizes phagocytic recognition for enhanced circulation times. As nanoparticles are functionalized with a human antibody fragment and produced with a polymer approved by FDA/EMA, it is expected nominal toxicity and well tolerated in humans.

Overall, NPs demonstrated adequate physical and technological characteristics. v6 Fab-PLGA-PEG NPs presented a size around 250 nm for empty PLGA-PEG NPs and 350 nm for bevacizumab-loaded PLGA-PEG NPs and an overall surface charge negative close to neutral. Empty PLGA-PEG NPs showed greater uniformity in size as they have lower PdI values. Functionalized and bevacizumab-loaded PLGA-PEG NPs had higher PdI values which means size heterogeneity. Since the AE of bevacizumab was ~80% with a DL of 7%, a low number of particles is necessary to cellular delivery of the bevacizumab and in this way, the toxicity of the therapy will be lower that when administrated free bevacizumab.

Overall, the formulations did not show cytotoxicity at the concentrations tested, for these cells.

NPs decorated with v6 Fab seemed to bind specifically to CD44v6 on the surface of cells, with a lower binding to cells that do not express CD44v6. Encapsulation of bevacizumab do not alter the specificity of v6 Fab-PLGA-PEG NPs to CD44v6 expressing cells. Bare and (-) Fab PLGA-PEG NPs showed a lower binding, and this probably confirms the specificity of v6 Fab to CD44v6 receptor.

The results of internalization and intracellular staining studies showed that the uptake of functionalized NPs did not occur due to unspecific interactions between the Fabs and the cells. The functionalization of the PLGA-PEG NPs with the v6 Fab allowed a higher uptake by the cells, when compared with non-functionalized NPs, confirming that the v6 Fab-PLGA-PEG NPs loaded with bevacizumab were specific for the cell-surface receptor CD44v6 and allowed an effective antibody intracellular delivery. To further support these results, it would be necessary add later times points to the study. Also, an *in vitro* release study could be done to observe the release profile of the drug from v6 Fab-PLGA-PEG NPs.

In this work it was showed that v6 Fab-PLGA-PEG NPs have the potential to deliver bevacizumab in CD44v6 expressing cancer cells. This target delivery system may result in higher bioavailability of a therapeutic agent at its site of action, that simultaneously increases the effectiveness of the drug, reduce the total dose needed and the side effects associated with the drug. It was demonstrated that it is possible to encapsulate a mAb in PLGA-PEG NPs and then functionalize with an antibody fragment for a specific and effective intracellular delivery of the drug. The nanocarrier developed in this dissertation present clinical potential and provide a launching point for future improvements and therapeutic and/or diagnostic opportunities. Though, its use in drug delivery requires further investigation and optimization.

2. Future Perspectives

The targeted nanosystem developed here can be optimized in different parameters. A release profile of the encapsulated drug can be done to study how the bevacizumab are released over time through PLGA-PEG NPs functionalized with a Fab. Also, it could be study if the Fab is dissociated of the surface of NPs along time.

Other nanocarriers can be developed based in this work, namely NPs loaded with mAbs with different chemical and/or biological properties and be applied in treatment or

diagnostic for other types of cancer or other diseases. Similarly, as NPs were functionalized with maleimide-thiol reaction, it is possible to conjugate the NPs to other ligands or other Fabs against different molecular targets.

NPs produced here were incorporated with a fluorescent dye (FKR648), which allows in a future work monitoring the systemic delivery of NPs in real time, in tumors with and without overexpression of CD44v6. In this way, it would be possible treat and monitor, at the same time, the progression of a tumor.

Lastly, as NPs were produced in low quantities, other methodologies with a higher output of production can be explored. For example, microfluidic platforms have been developed to scaling up the systems [153, 154].

References

[1] F. Bray, J. Ferlay, I. Soerjomataram, R.L. Siegel, L.A. Torre, A. Jemal, Global cancer statistics 2018: GLOBOCAN estimates of incidence and mortality worldwide for 36 cancers in 185 countries, CA Cancer J Clin (1542-4863) (2018).

[2] E.R. Fearon, B. Vogelstein, A genetic model for colorectal tumorigenesis, Cell 61(5) (1990) 759-767.

[3] E.R. Fearon, Molecular Genetics of Colorectal Cancer, Annu Rev Phatol 6(1) (2011) 479-507.

[4] K.F. Newton, J. Newman W Fau - Hill, J. Hill, Review of biomarkers in colorectal cancer, Colorectal Dis (2012) 3-17.

[5] K. Tariq, K. Ghias, Colorectal cancer carcinogenesis: a review of mechanisms, Cancer Biol Med 13(1) (2016) 120-135.

[6] L. Kotelevets, E. Chastre, D. Desmaele, P. Couvreur, Nanotechnologies for the treatment of colon cancer: From old drugs to new hope, Int J Pharm 514(1) (2016) 24-40.

[7] S.N. Thibodeau, A.J. French, J.M. Cunningham, D. Tester, L.J. Burgart, P.C. Roche, S.K. McDonnell, D.J. Schaid, C.W. Vockley, V.V. Michels, G.H. Farr, M.J. Connell, Microsatellite Instability in Colorectal Cancer: Different Mutator Phenotypes and the Principal Involvement of hMLH1, Cancer Res 58(8) (1998) 1713-1718.

[8] M. Toyota, N. Ahuja, M. Ohe-Toyota, J.B. Herman, S.B. Baylin, J.P. Issa, CpG island methylator phenotype in colorectal cancer, Proc Natl Acad Sci USA 96 (1999) 8681-8686.

[9] D.J. Weisenberger, K.D. Siegmund, M. Campan, J. Young, T.I. Long, M.A. Faasse, G.H. Kang, M. Widschwendter, D. Weener, D. Buchanan, H. Koh, L. Simms, M. Barker, B. Leggett, J. Levine, M. Kim, A.J. French, S.N. Thibodeau, J. Jass, R. Haile, P.W. Laird, CpG island methylator phenotype underlies sporadic microsatellite instability and is tightly associated with BRAF mutation in colorectal cancer, Nat Genet (1061-4036) (2006) 787-793.

[10] J. Lim, J.P. Thiery, Epithelial-mesenchymal transitions: insights from development, Development 139(19) (2012) 3471-3486.

[11] S. Heerboth, G. Housman, M. Leary, M. Longacre, S. Byler, K. Lapinska, A. Willbanks, S. Sarkar, EMT and tumor metastasis, Clin Transl Med 4 (2015) 1-13.

[12] J.P. Thiery, Epithelial-mesenchymal transitions in tumour progression, Nat Rev Cancer 2(6) (2002) 442-454.

[13] F. Arlt, U. Stein, Colon cancer metastasis: MACC1 and Met as metastatic pacemakers, Int J Biochem Cell Biol 41(12) (2009) 2356-2359.

[14] U. Stein, P.M. Schlag, Clinical, Biological, and Molecular Aspects of Metastasis in Colorectal Cancer, in: M. Dietel (Ed.), Targeted Therapies in Cancer, Springer Berlin Heidelberg, Berlin, Heidelberg, 2007, pp. 61-80.

[15] F. Arvelo, F. Sojo, C. Cotte, Biology of colorectal cancer, Ecancermedicalscience 9 (2015) 1-20.

[16] P. Dalerba, S.J. Dylla, I.K. Park, R. Liu, X. Wang, R.W. Cho, T. Hoey, A. Gurney, E.H. Huang, D.M. Simeone, A.A. Shelton, G. Parmiani, C. Castelli, M.F. Clarke, Phenotypic characterization of human colorectal cancer stem cells, Proc Natl Acad Sci USA (0027-8424) (2007) 10158-10163.

[17] H. Brenner, M. Kloor, C. Pox, Colorectal cancer, The Lancet 383(9927) (2014) 1490-1502.

[18] A. Anitha, S. Maya, A.J. Sivaram, U. Mony, R. Jayakumar, Combinatorial nanomedicines for colon cancer therapy, Wiley Interdiscipl Rev Nanomed Nanobiotechnol 8(1) (2016) 151-159.

[19] B. Viswanath, S. Kim, K. Lee, Recent insights into nanotechnology development for detection and treatment of colorectal cancer, Int J Nanomedicine 11 (2016) 2491-2504.

[20] R. Labianca, B. Nordlinger, G.D. Beretta, S. Mosconi, M. Mandala, A. Cervantes, D. Arnold, E.G.W. Group, Early colon cancer: ESMO Clinical Practice Guidelines for diagnosis, treatment and follow-up, Ann Oncol 24 Suppl 6 (2013) 64-72.

[21] E. Van Cutsem, A. Cervantes, R. Adam, A. Sobrero, J.H. Van Krieken, D. Aderka, E. Aranda Aguilar, A. Bardelli, A. Benson, G. Bodoky, F. Ciardiello, A. D'Hoore, E. Diaz-Rubio, J.Y. Douillard, M. Ducreux, A. Falcone, A. Grothey, T. Gruenberger, K. Haustermans, V. Heinemann, P. Hoff, C.H. Kohne, R. Labianca, P. Laurent-Puig, B. Ma, T. Maughan, K. Muro, N. Normanno, P. Osterlund, W.J. Oyen, D. Papamichael, G. Pentheroudakis, P. Pfeiffer, T.J. Price, C. Punt, J. Ricke, A. Roth, R. Salazar, W. Scheithauer, H.J. Schmoll, J. Tabernero, J. Taieb, S. Tejpar, H. Wasan, T. Yoshino, A. Zaanan, D. Arnold, ESMO consensus guidelines for the management of patients with metastatic colorectal cancer, Ann Oncol 27(8) (2016) 1386-1422.

[22] M.R. Hasan, S.H. Ho, D.A. Owen, I.T. Tai, Inhibition of VEGF induces cellular senescence in colorectal cancer cells, Int J Cancer 129(9) (2011) 2115-2123.

[23] E. Van Cutsem, C.H. Köhne, E. Hitre, Zaluski, C.R. Chang Chien, A. Makhson, G. D'Haens, T. Pintér, R. Lim, G. Bodoky, J.K. Roh, G. Folprecht, P. Ruff, C. Stroh, S. Tejpar, M. Schlichting, J. Nippgen, P. Rougier, Cetuximab and Chemotherapy as Initial Treatment for Metastatic Colorectal Cancer, N Engl J Med 360(14) (2009) 1408-1417.

[24] M. Peeters, T.J. Price, A. Cervantes, A.F. Sobrero, M. Ducreux, Y. Hotko, T. Andre, E. Chan, F. Lordick, C.J. Punt, A.H. Strickland, G. Wilson, T.E. Ciuleanu, L. Roman, E. Van Cutsem, V. Tzekova, S. Collins, K.S. Oliner, A. Rong, J. Gansert, Randomized phase III study of panitumumab with fluorouracil, leucovorin, and irinotecan (FOLFIRI) compared with FOLFIRI alone as second-line treatment in patients with metastatic colorectal cancer, J Clin Oncol 28(31) (2010) 4706-4713.

[25] H. Hurwitz, L. Fehrenbacher, W. Novotny, T. Cartwright, J. Hainsworth, W. Heim, J. Berlin, A. Baron, S. Griffing, E. Holmgren, N. Ferrara, G. Fyfe, B. Rogers, R. Ross, F. Kabbinavar, Bevacizumab plus Irinotecan, Fluorouracil, and Leucovorin for Metastatic Colorectal Cancer, N Engl J Med 350(23) (2004) 2335-2342.

[26] A. Lièvre, E. Samalin, E. Mitry, E. Assenat, C. Boyer-Gestin, C. Lepère, J.B. Bachet, F. Portales, J.N. Vaillant, M. Ychou, P. Rougier, Bevacizumab plus FOLFIRI or FOLFOX in chemotherapy-refractory patients with metastatic colorectal cancer: a retrospective study, BMC Cancer 9(1) (2009).

[27] C. Cremolini, F. Loupakis, C. Antoniotti, C. Lupi, E. Sensi, S. Lonardi, S. Mezi, G. Tomasello, M. Ronzoni, A. Zaniboni, G. Tonini, C. Carlomagno, G. Allegrini, S. Chiara, M. D'Amico, C. Granetto, M. Cazzaniga, L. Boni, G. Fontanini, A. Falcone, FOLFOXIRI plus bevacizumab versus FOLFIRI plus bevacizumab as first-line treatment of patients with metastatic colorectal cancer: updated overall survival and molecular subgroup analyses of the open-label, phase 3 TRIBE study, Lancet Oncol 16(13) (2015) 1306-1315.

[28] H. Maeda, The enhanced permeability and retention (EPR) effect in tumor vasculature: the key role of tumor-selective macromolecular drug targeting, Adv Enzyme Regul (0065-2571) (2001) 189-207.

[29] S.D. Steichen, M. Caldorera-Moore, N.A. Peppas, A review of current nanoparticle and targeting moieties for the delivery of cancer therapeutics, Eur J Pharm Sci 48(3) (2013) 416-427.

[30] I. Morath, T.N. Hartmann, V. Orian-Rousseau, CD44: More than a mere stem cell marker, Int J Biochem Cell Biol 81(Pt A) (2016) 166-173.

[31] V. Orian-Rousseau, CD44 Acts as a Signaling Platform Controlling Tumor Progression and Metastasis, Front Immunol 6 (2015) 1-4.

[32] V. Orian-Rousseau, CD44, a therapeutic target for metastasising tumours, Eur J Cancer 46(7) (2010) 1271-1277.

[33] M. Zoller, CD44: can a cancer-initiating cell profit from an abundantly expressed molecule?, Nat Rev Cancer 11(4) (2011) 254-267.

[34] L. Prochazka, R. Tesarik, J. Turanek, Regulation of alternative splicing of CD44 in cancer, Cell Signal 26(10) (2014) 2234-2239.

[35] V. Orian-Rousseau, J. Sleeman, CD44 is a multidomain signaling platform that integrates extracellular matrix cues with growth factor and cytokine signals, Adv Cancer Res 123 (2014) 231-254.

[36] V. Wielenga, K.-H. Heider, G. Johan, A. Offerhaus, G. Adolf, F. van den Berg, H. Ponta, P. Herrlich, S. Pals, Expression of CD44 variant proteins in human colorectal cancer is related to tumor progression, Cancer Research 53 (1993) 4754-4756.

[37] U. Günthert, M. Hofmann, W. Rudy, S. Reber, M. Zöller, I. Hauβmann, S. Matzku, A. Wenzel, H. Ponta, P. Herrlich, A new variant of glycoprotein CD44 confers metastatic potential to rat carcinoma cells, Cell 65(1) (1991) 13-24.

[38] S. Seiter, W. Tilgen, K. Herrman, D. Schadendorf, E. Patzelt, P. Moller, M. Zoller, Expression of CD44 splice variants in human skin and epidermal tumors, Virchows Arch 428 (1996) 141-149.

[39] M. Todaro, M. Gaggianesi, V. Catalano, A. Benfante, F. Iovino, M. Biffoni, T. Apuzzo, I. Sperduti, S. Volpe, G. Cocorullo, G. Gulotta, F. Dieli, R. De Maria, G. Stassi, CD44v6 is

a marker of constitutive and reprogrammed cancer stem cells driving colon cancer metastasis, Cell Stem Cell 14(3) (2014) 342-356.

[40] S. Hasenauer, D. Malinger, D. Koschut, G. Pace, A. Matzke, A. von Au, V. Orian-Rousseau, Internalization of Met requires the co-receptor CD44v6 and its link to ERM proteins, PLoS One 8(4) (2013) 1-15.

[41] V. Orian-Rousseau, L. Chen, J.P. Sleeman, P. Herrlich, H. Ponta, CD44 is required for two consecutive steps in HGF/c-Met signaling, Genes Dev 16(23) (2002) 3074-3086.

[42] V. Orian-Rousseau, H. Morrison, A. Matzke, T. Kastilan, G. Pace, P. Herrlich, H. Ponta, Hepatocyte growth factor-induced Ras activation requires ERM proteins linked to both CD44v6 and F-actin, Mol Biol Cell 18(1) (2007) 76-83.

[43] C. Cheng, M.B. Yaffe, P.A. Sharp, A positive feedback loop couples Ras activation and CD44 alternative splicing, Genes Dev 20(13) (2006) 1715-1720.

[44] N. Ferrara, VEGF and the quest for tumour angiogenesis factors, Nat Rev Cancer 2(10) (2002) 795-803.

[45] M. Tremmel, A. Matzke, I. Albrecht, A.M. Laib, V. Olaku, K. Ballmer-Hofer, G. Christofori, M. Heroult, H.G. Augustin, H. Ponta, V. Orian-Rousseau, A CD44v6 peptide reveals a role of CD44 in VEGFR-2 signaling and angiogenesis, Blood 114(25) (2009) 5236-5244.

[46] C.B. da Cunha, C. Oliveira, X. Wen, B. Gomes, S. Sousa, G. Suriano, M. Grellier, D.G. Huntsman, F. Carneiro, P.L. Granja, R. Seruca, De novo expression of CD44 variants in sporadic and hereditary gastric cancer, Lab Invest 90(11) (2010) 1604-1614.

[47] F. Carneiro, D.G. Huntsman, T.C. Smyrk, D.A. Owen, R. Seruca, P. Pharoah, C. Caldas, M. Sobrinho-Simoes, Model of the early development of diffuse gastric cancer in E-cadherin mutation carriers and its implications for patient screening, J Pathol 203(2) (2004) 681-687.

[48] B.M. Tijink, J. Buter, R. de Bree, G. Giaccone, M.S. Lang, A. Staab, C.R. Leemans, G.A. van Dongen, A phase I dose escalation study with anti-CD44v6 bivatuzumab mertansine in patients with incurable squamous cell carcinoma of the head and neck or esophagus, Clin Cancer Res (1078-0432) (2006) 6064-6072.

[49] A. Matzke, P. Herrlich, H. Ponta, V. Orian-Rousseau, A Five-Amino-Acid Peptide Blocks Met- and Ron-Dependent Cell Migration, Cancer Res 65(14) (2005) 6105-6110.

[50] A. Matzke-Ogi, K. Jannasch, M. Shatirishvili, B. Fuchs, S. Chiblak, J. Morton, B. Tawk, T. Lindner, O. Sansom, F. Alves, A. Warth, C. Schwager, W. Mier, J. Kleeff, H. Ponta, A. Abdollahi, V. Orian-Rousseau, Inhibition of Tumor Growth and Metastasis in Pancreatic Cancer Models by Interference With CD44v6 Signaling, Gastroenterology 150(2) (2016) 513-525.

[51] K. Sandstrom, A.K. Haylock, D. Spiegelberg, F. Qvarnstrom, K. Wester, M. Nestor, A novel CD44v6 targeting antibody fragment with improved tumor-to-blood ratio, Int J Oncol 40(5) (2012) 1525-1532.

[52] A. Knappik, L. Ge, A. Honegger, P. Pack, M. Fischer, G. Wellnhofer, A. Hoess, J. Wölle, A. Plückthun, B. Virnekäs, Fully synthetic human combinatorial antibody libraries (HuCAL) based on modular consensus frameworks and CDRs randomized with trinucleotides, J Mol Biol 296(1) (2000) 57-86.

[53] J. Prassler, S. Thiel, C. Pracht, A. Polzer, S. Peters, M. Bauer, S. Norenberg, Y. Stark, J. Kolln, A. Popp, S. Urlinger, M. Enzelberger, HuCAL PLATINUM, a synthetic Fab library optimized for sequence diversity and superior performance in mammalian expression systems, J Mol Biol 413(1) (2011) 261-278.

[54] A.K. Haylock, D. Spiegelberg, J. Nilvebrant, K. Sandstrom, M. Nestor, In vivo characterization of the novel CD44v6-targeting Fab fragment AbD15179 for molecular imaging of squamous cell carcinoma: a dual-isotope study, EJNMMI Res (2191-219X) (2014) 1-13.

[55] A.K. Haylock, D. Spiegelberg, A.C. Mortensen, R.K. Selvaraju, J. Nilvebrant, O. Eriksson, V. Tolmachev, M.V. Nestor, Evaluation of a novel type of imaging probe based on a recombinant bivalent mini-antibody construct for detection of CD44v6-expressing squamous cell carcinoma, Int J Oncol 48(2) (2016) 461-470.

[56] P.J. Kennedy, F. Sousa, D. Ferreira, C. Pereira, M. Nestor, C. Oliveira, P.L. Granja, B. Sarmento, Fab-conjugated PLGA nanoparticles effectively target cancer cells expressing human CD44v6, Acta Biomater 81 (2018) 208-218.

[57] M. Ferrari, Cancer nanotechnology: opportunities and challenges, Nat Rev Cancer 5(3) (2005) 161-171.

[58] J. Shi, P.W. Kantoff, R. Wooster, O.C. Farokhzad, Cancer nanomedicine: progress, challenges and opportunities, Nat Rev Cancer 17(1) (2017) 20-37.

[59] V.P. Torchilin, Targeted pharmaceutical nanocarriers for cancer therapy and imaging, AAPS J (1550-7416) (2007) E128-147.

[60] P. Sharma, S. Brown, G. Walter, S. Santra, B. Moudgil, Nanoparticles for bioimaging, Adv Colloid Interface Sci 123-126 (2006) 471-485.

[61] H. Maeda, Toward a full understanding of the EPR effect in primary and metastatic tumors as well as issues related to its heterogeneity, Adv Drug Deliv Rev (1872-8294) (2015) 1-4.

[62] D.A. Richards, A. Maruani, V. Chudasama, Antibody fragments as nanoparticle targeting ligands: a step in the right direction, Chem Sci 8(1) (2017) 63-77.

[63] A. des Rieux, V. Fievez, M. Garinot, Y.J. Schneider, V. Preat, Nanoparticles as potential oral delivery systems of proteins and vaccines: a mechanistic approach, J Control Release 116(1) (2006) 1-27.

[64] R. Singh, J.W. Lillard, Jr., Nanoparticle-based targeted drug delivery, Exp Mol Pathol 86(3) (2009) 215-223.

[65] S. Sharma, A. Parmar, S. Kori, R. Sandhir, PLGA-based nanoparticles: A new paradigm in biomedical applications, TrAC Trends in Analytical Chemistry 80 (2016) 30-40.

[66] C. Martins, F. Sousa, F. Araujo, B. Sarmento, Functionalizing PLGA and PLGA Derivatives for Drug Delivery and Tissue Regeneration Applications, Adv Healthc Mater 7(1) (2018) 1-24.

[67] C. Azevedo, M.H. Macedo, B. Sarmento, Strategies for the enhanced intracellular delivery of nanomaterials, Drug Discov Today 23(5) (2018) 944-959.

[68] N. Kamaly, Z. Xiao, P.M. Valencia, A.F. Radovic-Moreno, O.C. Farokhzad, Targeted polymeric therapeutic nanoparticles: design, development and clinical translation, Chem Soc Rev 41(7) (2012) 2971-3010.

[69] F. Danhier, E. Ansorena, J.M. Silva, R. Coco, A. Le Breton, V. Preat, PLGA-based nanoparticles: an overview of biomedical applications, J Control Release 161(2) (2012) 505-522.

[70] J.S. Suk, Q. Xu, N. Kim, J. Hanes, L.M. Ensign, PEGylation as a strategy for improving nanoparticle-based drug and gene delivery, Adv Drug Deliv Rev 99(Pt A) (2016) 28-51.

[71] G.T. Hermanson, Chapter 18 - PEGylation and Synthetic Polymer Modification, in: G.T. Hermanson (Ed.), Bioconjugate Techniques (Third Edition), Academic Press, Boston, 2013, pp. 787-838.

[72] Y. Barenholz, Doxil(R)-the first FDA-approved nano-drug: lessons learned, J Control Release 160(2) (2012) 117-134.

[73] B.A. Cisterna, N. Kamaly, W.I. Choi, A. Tavakkoli, O.C. Farokhzad, C. Vilos, Targeted nanoparticles for colorectal cancer, Nanomedicine (Lond) (1748-6963) (2016) 2443-2456.

[74] C.L. Ventola, Progress in Nanomedicine: Approved and Investigational Nanodrugs, P T 42(12) (2017) 742-755.

[75] J.A. Silverman, S.R. Deitcher, Marqibo® (vincristine sulfate liposome injection) improves the pharmacokinetics and pharmacodynamics of vincristine, Cancer Chemother Pharmacol 71(3) (2013) 555-564.

[76] Celator Pharmaceuticals, Inc. Celator announces phase 3 trial for VYXEOS™ (CPX-351) in patients with high-risk acute myeloid leukemia demonstrates statistically significant improvement in overall survival, 2016. http://www.prnewswire.com/news-releases/celator-announces-phase-3-trial-for-vyxeos-cpx-351-in-patients-with-high-risk-acute-myeloid-leukemia-demonstrates-statistically-significant-improvement-in-overall-survival-300235620.html. 2019).

[77] J. Carnevale, A.H. Ko, MM-398 (nanoliposomal irinotecan): emergence of a novel therapy for the treatment of advanced pancreatic cancer, Future Oncol (1744-8301) (2016) 453-464.

[78] U.S. Food and Drug Administration. Eligard (Leuprolide Acetate) Injectable Suspension, 2006. http://www.accessdata.fda.gov/drugsatfda_docs/nda/2004/021731s000_EligardTOC.cfm. 2019).

[79] P.A. Dinndorf, J. Gootenberg, M.H. Cohen, P. Keegan, R. Pazdur, FDA drug approval summary: pegaspargase (oncaspar) for the first-line treatment of children with acute lymphoblastic leukemia (ALL), Oncologist (1083-7159) (2007) 991-998.

[80] K. Ando, K. Mori, N. Corradini, F. Redini, D. Heymann, Mifamurtide for the treatment of nonmetastatic osteosarcoma, Expert Opin Pharmacother (1744-7666) (2011) 285-292.

[81] R.C. Leonard, S. Williams, A. Tulpule, A.M. Levine, S. Oliveros, Improving the therapeutic index of anthracycline chemotherapy: focus on liposomal doxorubicin (Myocet), Breast (1532-3080) (2009) 218-224.

[82] Clinical trials database: NCT00361842 2012. https://clinicaltrials.gov/ct2/show/NCT00361842. 2019).

[83] K.J. Chen, E. Chaung, S.P. Wey, K.J. Lin, Cheng, C.C. Lin, H.I. Liu, H.W. Tseng, C. Liu, M.C. Wei, C.M. Liu, H.W. Sung, Hyperthermia-mediated local drug delivery by a bubble-generating liposomal system for tumor-specific chemotherapy, ACS Nano (1936-086X) (2014) 5105-5115.

[84] D. Sutton, N. Nasongkla, E. Blanco, J. Gao, Functionalized micellar systems for cancer targeted drug delivery, Pharm Res (0724-8741) (2007) 1029-1046.

[85] T. Hamaguchi, Y. Matsumura, M. Suzuki, K. Shimizu, R. Goda, I. Nakamura, I. Nakatomi, M. Yokoyama, K. Kataoka, T. Kakizoe, NK105, a paclitaxel-incorporating micellar nanoparticle formulation, can extend in vivo antitumour activity and reduce the neurotoxicity of paclitaxel, Br J Cancer (0007-0920) (2005) 1240-1246.

[86] A.Z. Wang, F. Gu, L. Zhang, J.M. Chan, A. Radovic-Moreno, M.R. Shaikh, O.C. Farokhzad, Biofunctionalized targeted nanoparticles for therapeutic applications, Expert Opin Biol Ther 8(8) (2008) 1063-1070.

[87] N. Bertrand, J. Wu, X. Xu, N. Kamaly, O.C. Farokhzad, Cancer nanotechnology: the impact of passive and active targeting in the era of modern cancer biology, Adv Drug Deliv Rev 66 (2014) 2-25.

[88] Y.H. Bae, K. Park, Targeted drug delivery to tumors: myths, reality and possibility, J Control Release 153(3) (2011) 198-205.

[89] D. Peer, J.M. Karp, S. Hong, O.C. Farokhzad, R. Margalit, R. Langer, Nanocarriers as an emerging platform for cancer therapy, Nat Nanotechnol (1748-3395) (2007) 751-760.

[90] J. Panyam, V. Labhasetwar, Biodegradable nanoparticles for drug and gene delivery to cells and tissue, Adv Drug Deliv Rev 55(3) (2003) 329-347.

[91] A. Jhaveri, V. Torchilin, Intracellular delivery of nanocarriers and targeting to subcellular organelles, Expert Opin Drug Deliv (1744-7593) (2016) 49-70.

[92] J. Panyam, W.Z. Zhou, S. Prabha, S.K. Sahoo, V. Labhasetwar, Rapid endo-lysosomal escape of poly(DL-lactide-co-glycolide) nanoparticles: implications for drug and gene delivery, FASEB J (1530-6860) (2002) 1217-1226.

[93] O. Boussif, M. Zanta, J.P. Behr, Optimized galenics improve in vitro gene transfer with cationic molecules up to 1000-fold, Gene Ther (0969-7128) (1996) 1074-1080.

[94] D.S. Kohane, Microparticles and nanoparticles for drug delivery, Biotechnol Bioeng 96(2) (2007) 203-209.

[95] R.J. Harris, B. Kabakoff, F.D. Macchi, F.J. Shen, M. Kwong, J.D. Andya, S.J. Shire, N. Bjork, K. Totpal, A.B. Chen, Identification of multiple sources of charge heterogeneity in a recombinant antibody, J Chromatogr B Biomed Sci Appl (2001) 1387-2273.

[96] P.J. Kennedy, C. Oliveira, P.L. Granja, B. Sarmento, Antibodies and associates: Partners in targeted drug delivery, Pharmacol Ther 177 (2017) 129-145.

[97] T.M. Allen, Ligand-targeted therapeutics in anticancer therapy, Nat Rev Cancer 2(10) (2002) 750-763.

[98] M.M. Cardoso, I.N. Peca, A.C.A. Roque, Antibody-Conjugated Nanoparticles for Therapeutic Applications, Curr Med Chem 19(19) (2012) 3103-3127.

[99] A.C. Roque, C.R. Lowe, M.A. Taipa, Antibodies and genetically engineered related molecules: production and purification, Biotechnol Prog (8756-7938) (2004) 639-654.

[100] M. Arruebo, M. Valladares, Á. González-Fernández, Antibody-Conjugated Nanoparticles for Biomedical Applications, J Nanomater 2009 (2009) 1-24.

[101] H.W. Schroeder, Jr., L. Cavacini, Structure and function of immunoglobulins, J Allergy Clin Immunol (1097-6825) (2010) S41-52.

[102] P. Chames, M. Van Regenmortel, E. Weiss, D. Baty, Therapeutic antibodies: successes, limitations and hopes for the future, Br J Pharmacol 157(2) (2009) 220-233.

[103] C.T. Turner, S.J.P. McInnes, N.H. Voelcker, A.J. Cowin, Therapeutic Potential of Inorganic Nanoparticles for the Delivery of Monoclonal Antibodies, J Nanomater 2015 (2015) 1-11.

[104] P. Carter, Improving the efficacy of antibody-based cancer therapies, Nat Rev Cancer (1474-175X) (2001) 118-129.

[105] L. Martínez-Jothar, S. Doulkeridou, R.M. Schiffelers, J. Sastre Torano, S. Oliveira, C.F. van Nostrum, W.E. Hennink, Insights into maleimide-thiol conjugation chemistry: Conditions for efficient surface functionalization of nanoparticles for receptor targeting, J Control Release 282 (2018) 101-109.

[106] A.R. Sousa, M.J. Oliveira, B. Sarmento, Impact of CEA-targeting Nanoparticles for Drug Delivery in Colorectal Cancer, J Pharmacol Exp Ther 370(3) (2019) 657-670.

[107] L. Nobs, F. Buchegger, R. Gurny, E. Allemann, Current methods for attaching targeting ligands to liposomes and nanoparticles, J Pharm Sci 93(8) (2004) 1980-1992.

[108] G.T. Hermanson, Chapter 2 - Functional Targets for Bioconjugation, in: G.T. Hermanson (Ed.), Bioconjugate Techniques (Third Edition), Academic Press, Boston, 2013, pp. 127-228.

[109] A.M. Scott, J.D. Wolchok, L.J. Old, Antibody therapy of cancer, Nat Rev Cancer 12 (2012) 278-287.

[110] M. Steinitz, Three decades of human monoclonal antibodies: past, present and future developments, Hum Antibodies 18(1-2) (2009) 1-10.

[111] H. Samaranayake, T. Wirth, D. Schenkwein, J.K. Räty, S. Ylä-Herttuala, Challenges in monoclonal antibody-based therapies Ann Med 41(5) (2009) 322-331.

[112] H. Modjtahedi, S. Ali, S. Essapen, Therapeutic application of monoclonal antibodies in cancer: advances and challenges, Br Med Bull 104 (2012) 41-59.

[113] R. Beckman, L. Weiner, H. Davis, Antibody constructs in cancer therapy, Cancer 109(2) (2007) 170-179.

[114] F. Sousa, P. Castro, P. Fonte, P.J. Kennedy, M.T. Neves-Petersen, B. Sarmento, Nanoparticles for the delivery of therapeutic antibodies: Dogma or promising strategy?, Expert Opin Drug Deliv 14(10) (2017) 1163-1176.

[115] S.H. Jang, M.G. Wientjes, D. Lu, J.L. Au, Drug delivery and transport to solid tumors, Pharm Res (0724-8741) (2003) 1337-1350.

[116] D.W. Grainger, Controlled-release and local delivery of therapeutic antibodies, Expert Opin Biol Ther 4(7) (2004) 1029-1044.

[117] A.R. Srinivasan, A. Lakshmikuttyamma, S.A. Shoyele, Investigation of the Stability and Cellular Uptake of Self-Associated Monoclonal Antibody (MAb) Nanoparticles by Non-Small Lung Cancer Cells, Mol Pharm 10(9) (2013) 3275-3284.

[118] R. Varshochian, M. Jeddi-Tehrani, A.R. Mahmoudi, M.R. Khoshayand, F. Atyabi, A. Sabzevari, M.R. Esfahani, R. Dinarvand, The protective effect of albumin on bevacizumab activity and stability in PLGA nanoparticles intended for retinal and choroidal neovascularization treatments, Eur J Pharm Sci 50(3) (2013) 341-352.

[119] D.M. Ecker, S.D. Jones, H.L. Levine, The therapeutic monoclonal antibody market, MAbs 7(1) (2015) 9-14.

[120] N. Ferrara, VEGF as a Therapeutic Target in Cancer, Oncology 69(suppl 3)(Suppl. 3) (2005) 11-16.

[121] L.D. Sasich, S.R. Sukkari, The US FDAs withdrawal of the breast cancer indication for Avastin (bevacizumab), Saudi Pharm J 20(4) (2012) 381-385.

[122] N. Ferrara, K.J. Hillan, H.P. Gerber, W. Novotny, Discovery and development of bevacizumab, an anti-VEGF antibody for treating cancer, Nat Rev Drug Discov 3 (2004) 391-400.

[123] Y. Wang, D. Fei, M. Vanderlaan, A. Song, Biological activity of bevacizumab, a humanized anti-VEGF antibody in vitro, Angiogenesis 7(4) (2004) 335-345.

[124] C.G. Willett, Y. Boucher, E. di Tomaso, D.G. Duda, L.L. Munn, R.T. Tong, D.C. Chung, D.V. Sahani, S.P. Kalva, S.V. Kozin, M. Mino, K.S. Cohen, D.T. Scadden, A.C. Hartford, A.J. Fischman, J.W. Clark, D.P. Ryan, A.X. Zhu, L.S. Blaszkowsky, H.X. Chen, P.C. Shellito, G.Y. Lauwers, R.K. Jain, Direct evidence that the VEGF-specific antibody bevacizumab has antivascular effects in human rectal cancer, Nat Med 10(2) (2004) 145-147.

[125] F. Li, B. Hurley, Y. Liu, B. Leonard, M. Griffith, Controlled release of bevacizumab through nanospheres for extended treatment of age-related macular degeneration, Open Ophthalmol J 6 (2012) 54-58.

[126] M. Abrishami, S. Zarei-Ghanavati, D. Sourosh, M. Rouhbakhsh, M. Jaafari, B. Malaekeh-nikouei, Preparation, characterization, and in vivo evaluation of nanoliposomes-encapsulated bevacizumab (avastin) for intravitreal administration, Retina (Philadelphia, Pa.) 29 (2009) 699-703.

[127] D. Schweizer, T. Serno, A. Goepferich, Controlled release of therapeutic antibody formats, Eur J Pharm Biopharm 88(2) (2014) 291-309.

[128] R.T. Penson, H.Q. Huang, L.B. Wenzel, B.J. Monk, S. Stockman, H.J. Long, L.M. Ramondetta, L.M. Landrum, A. Oaknin, T.J.A. Reid, M.M. Leitao, M. Method, H. Michael, K.S. Tewari, Bevacizumab for advanced cervical cancer: patient-reported outcomes of a randomised, phase 3 trial (NRG Oncology-Gynecologic Oncology Group protocol 240), Lancet Oncol 16(3) (2015) 301-311.

[129] P. Mésange, V. Poindessous, M. Sabbah, A.E. Escargueil, A. de Gramont, A.K. Larsen, Intrinsic bevacizumab resistance is associated with prolonged activation of autocrine VEGF signaling and hypoxia tolerance in colorectal cancer cells and can be overcome by nintedanib, a small molecule angiokinase inhibitor, Oncotarget 5(13) (2014) 4709-4721.

[130] F. Sousa, A. Cruz, P. Fonte, I.M. Pinto, M.T. Neves-Petersen, B. Sarmento, A new paradigm for antiangiogenic therapy through controlled release of bevacizumab from PLGA nanoparticles, Sci Rep 7(1) (2017) 1-13.

[131] T.U. Krohne, N. Eter, F.G. Holz, C.H. Meyer, Intraocular Pharmacokinetics of Bevacizumab After a Single Intravitreal Injection in Humans, Am J Ophthalmol 146(4) (2008) 508-512.

[132] K.M. Sampat, S.J. Garg, Complications of intravitreal injections, Curr Opin Ophthalmol 21(3) (2010) 178-183.

[133] Y. Lu, N. Zhou, X. Huang, J.W. Cheng, F.Q. Li, R.L. Wei, J.P. Cai, Effect of intravitreal injection of bevacizumab-chitosan nanoparticles on retina of diabetic rats, Int J Ophthalmol 7(1) (2014) 1-7.

[134] L. Battaglia, M. Gallarate, E. Peira, D. Chirio, I. Solazzi, S. Giordano, C. Gigliotti, C. Riganti, C. Dianzani, Bevacizumab loaded solid lipid nanoparticles prepared by the coacervation technique: preliminary in vitro studies, Nanotechnology 26(25) (2015) 1-11.

[135] J. Andrew, E. Anglin, E. Wu, M. Chen, L. Cheng, W. Freeman, M. Sailor, Sustained Release of a Monoclonal Antibody from Electrochemically Prepared Mesoporous Silicon Oxide, Adv Funct Mater 20(23) (2010) 4168-4174.

[136] P. Fonte, S. Soares, A. Costa, J. Andrade, V. Seabra, S. Reis, B. Sarmento, Effect of cryoprotectants on the porosity and stability of insulin-loaded PLGA nanoparticles after freeze-drying, Biomatter 2(4) (2012) 329-339.

[137] F. Sousa, A. Cruz, I.M. Pinto, B. Sarmento, Nanoparticles provide long-term stability of bevacizumab preserving its antiangiogenic activity, Acta Biomater 78 (2018) 285-295.

[138] P.J. Kennedy, I. Perreira, D. Ferreira, M. Nestor, C. Oliveira, P.L. Granja, B. Sarmento, Impact of surfactants on the target recognition of Fab-conjugated PLGA nanoparticles, Eur J Pharm Biopharm 127 (2018) 366-370.

[139] F. Sousa, V.M.F. Goncalves, B. Sarmento, Development and validation of a rapid reversed-phase HPLC method for the quantification of monoclonal antibody bevacizumab from polyester-based nanoparticles, J Pharm Biomed Anal 142 (2017) 171-177.

[140] G. Alter, J. Malenfant, M. Altfeld, CD107a as a functional marker for the identification of natural killer cell activity, J Immunol Methods (0022-1759) (2004) 15-22.

[141] S. Bhattacharjee, DLS and zeta potential – What they are and what they are not?, J Control Release 235 (2016) 337-351.

[142] Q. Xu, M. Nakajima, S. Ichikawa, N. Nakamura, P. Roy, H. Okadome, T. Shiina, Effects of surfactant and electrolyte concentrations on bubble formation and stabilization, J Colloid Interface Sci (1095-7103) (2009) 208-214.

[143] P. Rafiei, A. Haddadi, Docetaxel-loaded PLGA and PLGA-PEG nanoparticles for intravenous application: pharmacokinetics and biodistribution profile, Int J Nanomedicine 12 (2017) 935-947.

[144] S.M. Moghimi, A.C. Hunter, T.L. Andresen, Factors controlling nanoparticle pharmacokinetics: an integrated analysis and perspective, Annu Rev Pharmacol Toxicol 52 (2012) 481-503.

[145] H. Zhang, W. Cui, J. Bei, S. Wang, Preparation of poly(lactide-co-glycolide-co-caprolactone) nanoparticles and their degradation behaviour in aqueous solution, Polym Degrad Stabil 91(9) (2006) 1929-1936.

[146] D.E. Owens, 3rd, N.A. Peppas, Opsonization, biodistribution, and pharmacokinetics of polymeric nanoparticles, Int J Pharm 307(1) (2006) 93-102.

[147] F. Araujo, N. Shrestha, M.A. Shahbazi, P. Fonte, E.M. Makila, J.J. Salonen, J.T. Hirvonen, P.L. Granja, H.A. Santos, B. Sarmento, The impact of nanoparticles on the mucosal translocation and transport of GLP-1 across the intestinal epithelium, Biomaterials (1878-5905) (2014) 9199-9207.

[148] M.E. Werner, S. Karve, R. Sukumar, N.D. Cummings, J.A. Copp, R.C. Chen, T.T. Zhang, A.Z. Wang, Folate-targeted nanoparticle delivery of chemo- and radiotherapeutics for the treatment of ovarian cancer peritoneal metastasis, Biomaterials 32(33) (2011) 8548-8554.

[149] Y. Lu, P.S. Low, Folate-mediated delivery of macromolecular anticancer therapeutic agents, Adv Drug Deliv Rev 54(5) (2002) 675-693.

[150] O.C. Farokhzad, J. Cheng, B.A. Teply, I. Sherifi, S. Jon, P.W. Kantoff, J.P. Richie, R. Langer, Targeted nanoparticle-aptamer bioconjugates for cancer chemotherapy in vivo, Proc Natl Acad Sci USA 103(16) (2006) 6315-6320.

[151] J.W. Park, K. Hong, D.B. Kirpotin, G. Colbern, R. Shalaby, J. Baselga, Y. Shao, U.B. Nielsen, J.D. Marks, D. Moore, D. Papahadjopoulos, C.C. Benz, Anti-HER2

immunoliposomes: enhanced efficacy attributable to targeted delivery, Clin Cancer Res 8(4) (2002) 1172-1181.

[152] F. Sousa, H.K. Dhaliwal, F. Gattacceca, B. Sarmento, M.M. Amiji, Enhanced anti-angiogenic effects of bevacizumab in glioblastoma treatment upon intranasal administration in polymeric nanoparticles, J Control Release 309 (2019) 37-47.

[153] C. Martins, F. Araujo, M.J. Gomes, C. Fernandes, R. Nunes, W. Li, H.A. Santos, F. Borges, B. Sarmento, Using microfluidic platforms to develop CNS-targeted polymeric nanoparticles for HIV therapy, Eur J Pharm Biopharm (1873-3441) (2019) 111-124.

[154] C. Martins, B. Sarmento, Microfluidic Manufacturing of Multitargeted PLGA/PEG Nanoparticles for Delivery of Taxane Chemotherapeutics, in: K.K. Jain (Ed.), Drug Delivery Systems, Springer New York, New York, NY, 2020, pp. 213-224.

Supplementary Information

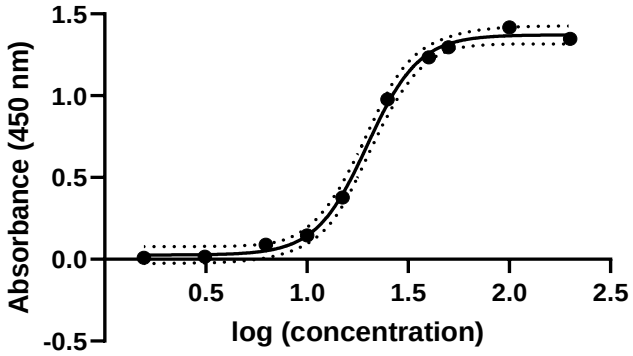

Figure S1. Standard curve of logarithmic v6 Fab standard concentrations (200, 100, 50, 40, 25, 15, 10, 6.25, 3.125 and 1.562 ng/µL). Black points represent the mean and dashed lines represent the standard deviation. n=3 replicates.

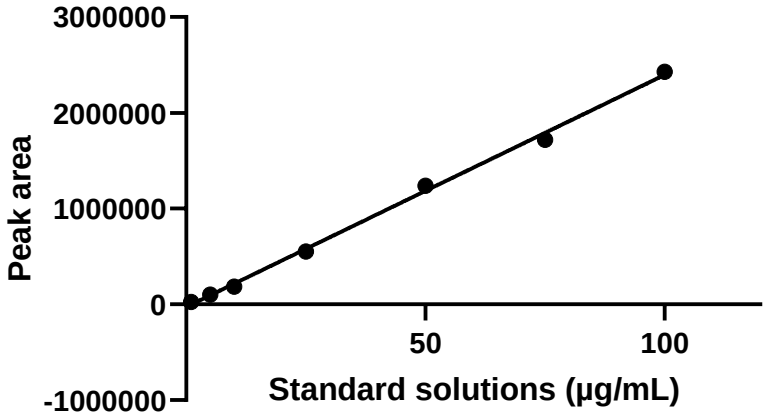

Figure S2. Standard curve of bevacizumab standard concentrations (1, 5, 10, 25, 50, 75 and 100 µg/mL). Black points represent mean of n=3 replicates.

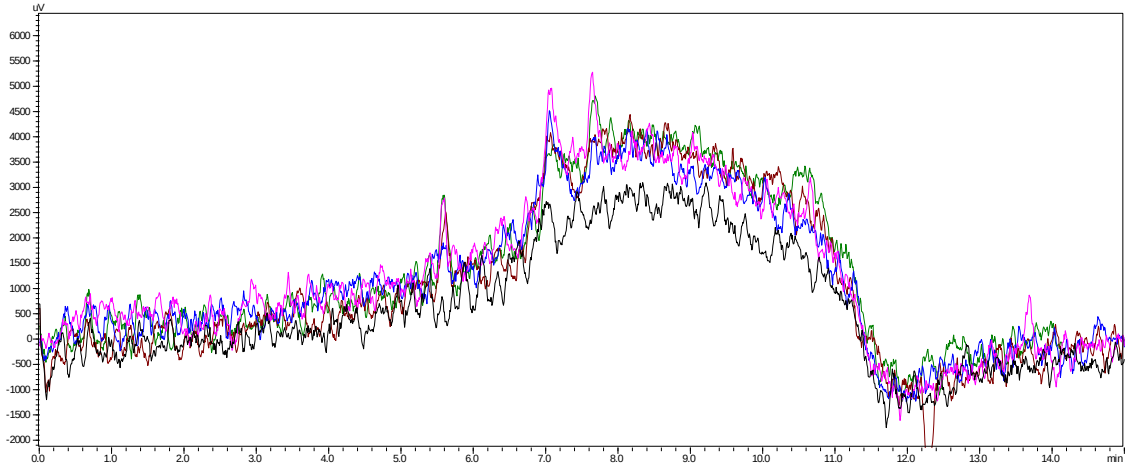

Figure S3. Chromatogram of a water sample and supernatants of bevacizumab-loaded PLGA-PEG NPs functionalized with v6 Fab analysed by RP-HPLC with fluorescence detection. Black line represents the water sample (n=1) and the pink, green, red and blue lines represent the supernatants of bevacizumab-loaded PLGA-PEG NPs functionalized with v6 Fab (n=4). Retention time at approximately 7.044 ± 0.006 minutes.

Acknowledgements

This dissertation was financed by the project NORTE-01-0145-FEDER-000012 by Norte Portugal Regional Operational Programme (NORTE 2020), and COMPETE 2020 - Operacional Programme for Competitiveness and Internationalisation (POCI), under the PORTUGAL 2020 Partnership Agreement, through the FEDER - Fundo Europeu de Desenvolvimento Regional, and by Portuguese funds through FCT - Fundação para a Ciência e a Tecnologia/Ministério da Ciência, Tecnologia e Ensino Superior in the framework of the project "Institute for Research and Innovation in Health Sciences" UID/BIM/04293/2019.